J. Fluid Mech. (2000), *vol.* 409, *pp.* 273–308. Printed in the United Kingdom

Surprises in viscous fingering

By S. TANVEER

Mathematics Department, The Ohio State University, Columbus, OH 43210, USA

(Received 1 June 1999 and in revised form 25 November 1999)

In this paper, we review some aspects of viscous fingering in a Hele-Shaw cell that at first sight appear to defy intuition. These include singular effects of surface tension relative to the corresponding zero-surface-tension problem both for the steady and unsteady problem. They also include a disproportionately large influence of small effects like local inhomogeneity of the flow field near the finger tip, or of the leakage term in boundary conditions that incorporate realistic thin-film effects. Through simple explicit model problems, we demonstrate how such properties are not unexpected for a system approaching structural instability or ill-posedness.

1. Introduction

A Hele-Shaw cell is a pair of parallel plates separated by a small gap b. The motion of a less viscous fluid displacing a more viscous fluid in a Hele-Shaw cell, effected by a pressure gradient, gravity or fluid injection, has been the subject of numerous investigations. An internet website compiled by Howison (see Howison 2000) lists more than six hundred references to investigations connected to Hele-Shaw flow. The reason for this intense interest is the mathematical relation to various problems in dendritic crystal growth, directional solidification, diffusion-limited aggregation, electrochemical growth (see discussions in Pelce 1988; Kessler, Koplik & Levine 1988), filtration combusion (Aldusin & Matkowsky 1998) and void electro-migration (Ben Amar 1999), though Darcian flow through a porous medium was the original motivation (Saffman & Taylor 1958).

In many Hele-Shaw cell studies to date, the geometry consists of a long rectilinear channel where the width of the cell is $2a$, with $b \ll a$ (figure 1). In this case, the interfacial motion is caused by an imposed pressure gradient which causes the more viscous fluid at infinity to be displaced with velocity V. Alternately, any gravity component parallel to the channel direction can effect interfacial displacement between two fluids of varying densities. Hele-Shaw flow has also been studied in radial and wedge geometries, where the interface moves due to injection of less viscous fluid or withdrawal of the more viscous fluid. However, in this paper, we will only be concerned with flow in a channel geometry, though there are some similar results for radial and wedge geometries (see for instance Thome *et al.* 1989; Combescot & Ben Amar 1991).

Here, we review some aspects of the Hele-Shaw flow that appear to defy physical intuition – hence the title of this paper. These include results for steady states, linear stability and the nonlinear initial value problem. We only review the literature as it relates to these particular aspects of Hele-Shaw flow. Over the years, many reviews have appeared from a range of perspectives (Saffman 1986; Bensimon *et al.* 1986; Homsy 1987; Pelce 1988; Kessler *et al.* 1988; Tanveer 1991; Hohlov 1990; Howison 1992). There are also many new and very interesting developments not found in

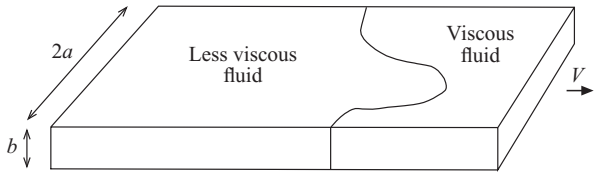

FIGURE 1. Hele-Shaw cell geometry.

any review that the author is familiar with. These involve complex fluids, phase-field models, surfactants, etc. and will not be discussed here.

The theme of the current paper is that apparently small effects are not always negligible. In connection with this theme, it is noteworthy that the following three-step procedure is commonly followed in all the physical sciences and engineering:

1. simplify equations by neglecting term(s);
2. find solutions to the resulting simplified equations in step 1;
3. justify neglect of term(s) in step 1 by estimating their sizes based on the solutions found in step 2.

If one can go through these steps successfully, it is usually assumed that the neglect of term(s) is not serious. What is implicit is the assumption that small terms in the equation (defined in the sense of step 3 above) can have only small effects on the solution, i.e. that the simplified equation is structurally stable. The notion of structural stability is well defined mathematically in the context of dynamical systems (see for example Guckenheimer & Holmes 1986). Without underlying structural stability, an equation cannot be assumed to be faithful to a real-world phenomenon, since approximations are always involved. If arbitrary small effects alter the solution structure, then it cannot be assumed that a particular solution to the idealized equation is necessarily physically relevant (observable in an experiment). One must consider the altered solution structure when previously neglected physical effects are introduced. When multiple small corrections are involved, it is not always sound to throw away terms that appear small in step 3 above. Rather, if solutions are analytic, the importance of a term is determined by its relative size in a neighbourhood of some point(s) in some complex domain, and whether its inclusion stabilizes the equation structurally. In problems involving multiple effects, the relative importance of terms can change as we approach a structurally unstable system. This causes changes in scalings, usually referred to as cross-overs. These ideas are illustrated here in a relatively simple linear example where explicit calculations can be performed, unlike the more complicated nonlinear Hele-Shaw equations. The simpler example serves as a useful vehicle in explaining the implications of many existing asymptotic and numerical results in steady Hele-Shaw fingering and two-dimensional dendritic crystal growth. In particular, it is pointed out why each of these problems, in the absence of a lateral curvature term in the interfacial conditions, forms a structurally unstable system. This is worth pointing out since this seems to be the source of some confusion in the literature.

In later sections of this paper, we describe some results for the nonlinear initial value problem for an evolving Hele-Shaw interface. The initial value problem for zero surface tension is known to be ill-posed (Howison 1986) in the sense that arbitrarily small differences in initial interface shape generally lead to radically different interface shapes, even a short time later. As with a stucturally unstable system, the solution to an ill-posed mathematical equation need not be physically meaningful (experimentally observable), since one does not have exact control over initial conditions in the real

world. Therefore, one cannot ascertain the physical relevance without considering how small regularization effects like surface tension alter the solution. For the Hele-Shaw initial value problem, it is known that there exists a family of explicit solutions to the ill-posed idealized problem that remain smooth for all times. This includes the ones by Saffman (1959) that evolve into a steady finger. A question relevant to the stated theme of this paper is whether, for any fixed time, such a smooth solution is the limit as surface tension tends to zero. We describe recent work (Tanveer 1993; Siegel, Tanveer & Dai 1996) that suggests that the answer is generally in the negative – that in an $O(1)$ time, the limiting solution veers off from the smooth idealized solution.

The paper is arranged as follows. In § 2, we describe some of the features observed in Hele-Shaw experiments. In § 3, we formulate mathematical equations and boundary conditions derived under some simplifying assumptions by McLean & Saffman (1981) (henceforth referred to as the MS equations). In § 4, we examine complications in interfacial boundary conditions due to thin-film effects, following previous work of Saffman (1982), Park & Homsy (1985) and Reinelt (1987*a*, *b*). Limits are examined when the corresponding boundary condition (SPHR) reduces to the simpler MS boundary conditions, at least formally. In § 5, we formulate the problem for a steady translating finger and point out the degeneracy of solution to the corresponding idealized problem with zero surface tension. We present an overview of results of many researchers that suggest that the steady solution set and its linear stability when surface tension tends to zero are different than for the idealized problem. We also describe results that suggest that solution properties for small surface tension can be sensitive to small perturbations near the finger tip or to thin-film corrections. In § 6, we demonstrate through an explicit example how seemingly surprising properties of steady fingers (and steady two-dimensional needle crystals) are entirely consistent with a system approaching structural instability. This example also illustrates the role of exponential asymptotics in steady-state selection. In § 7, we describe results to show that the limiting solution to an initial value problem, as surface tension tends to zero, need not be the corresponding solution to the idealized problem, even when the latter is smooth. We explain this result to be a consequence of the motion of surface-tension-induced singularities, clustered around a point (dubbed the 'daughter' singularity), towards the physical domain before any singularity of the idealized solution. The daughter singularity effect is demonstrated more explicitly in a model problem in § 8.

2. Experimental observations

It has been known since Hill (1952), Chuoke, van Meurs & van der Poel (1959) and Saffman & Taylor (1958) that a planar interface between a viscous fluid of viscosity μ displaced by a less viscous fluid of viscosity μ_1 ($\mu_1 < \mu$) is unstable. Saffman & Taylor (1958), in a classic paper, studied the finite stages of this instability in a rectilinear Hele-Shaw cell. It was found that a small disturbance grows; and after a transient stage of competition between fingers, a single stable steadily travelling finger with velocity U emerges for long times, except when the capillary effects are too small or equivalently the imposed pressure gradient (and therefore V) too large. The asymptotically steady finger shape and the corresponding flow in the lateral plane are sketched in figure 2, with lengths and velocities non-dimensionalized appropriately, and the flow shown in a frame where the finger is stationary.

The observed finger is symmetric about the channel centreline, as in figure 2, and has an asymptotic width of approximately one half the channel width ($\lambda \approx \frac{1}{2}$) for relatively larger values of capillary number $Ca = \mu V/T$ (T: surface tension) or small

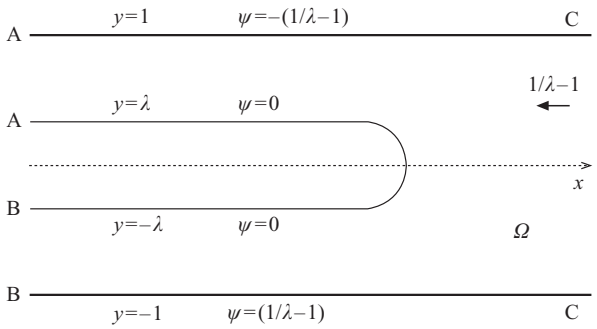

FIGURE 2. Steady finger and flow in the stationary finger frame.

values of gap-width to cell-width ratio $\epsilon = b/2a$. The Saffman–Taylor experiment has since been repeated by other investigators (Pitts 1980; Tabeling & Libchaber 1986; Tabeling, Zocchi & Libchaber 1987) and the dependence of the eventual finger width on the different control parameters documented more precisely. It has been found that the width of the steady finger relative to the channel width can be less than a half, and depends significantly on two independent parameters that may be taken as the gap to width ratio $\epsilon \equiv b/2a$ and the capillary number Ca. Further, it is found (Tabeling *et al.* 1987) that the interface is unstable when ϵ^2/Ca is smaller than some small critical value. This critical value seems to depend on the noise level in the experiment as well as on ϵ. The instability at very small values of ϵ^2/Ca leads to an intrinsically time-dependent (Tabeling *et al.* 1987; Maxworthy 1987; Arneodo *et al.* 1989) pattern of tip splitting and side branching that can lead to the development of an apparently fractal pattern over a range of length scales.

Another important experimental observation is the extreme sensitivity of the interfacial shapes to local flow inhomogeneities such as a little bubble (Couder, Gerard & Rabaud 1986) near the tip of a finger, a needle (Zocchi *et al.* 1987) piercing the interface, or anisotropy (Ben-Jacob *et al.* 1985) introduced by etching the glass plates. Such a local perturbation leads to narrower and more stable fingers than the regular ones. When instability does set in for these fingers, it is dendritic rather than the usual tip splitting. To a remarkable degree, these perturbed fingers resemble observed features of a needle crystal.

3. Equations and simplified boundary conditions

For convenience of presentation, we make a few simplifying assumptions. We assume the viscosity of the less viscous fluid to be zero. Further, we ignore gravity effects. It is to be noted for the simplest interfacial boundary conditions, as will be derived shortly, that the steady flow in a channel geometry with gravity parallel to the channel and non-zero viscosity ratio can be mathematically transformed (Saffman & Taylor 1958) to a flow where each is ignored. Further, as originally assumed by Saffman & Taylor (1958) and later by McLean & Saffman (1981), the less viscous fluid completely expels the more viscous fluid and the interface between the two fluids has a constant curvature in the transverse (narrow-gap) plane (figure 3). Experimental observations (see for instance, Tabeling & Libchaber 1986) suggest that this assumption is not realistic. Instead, a thin film of the more viscous fluid is likely to lubricate the gap walls as the less viscous fluid advances. We will discuss the thin-film complications in more detail in the next section.

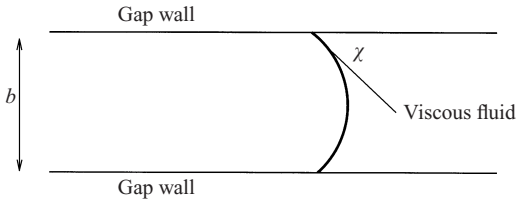

FIGURE 3. Assumed interface shape in the narrow-gap plane for MS boundary conditions.

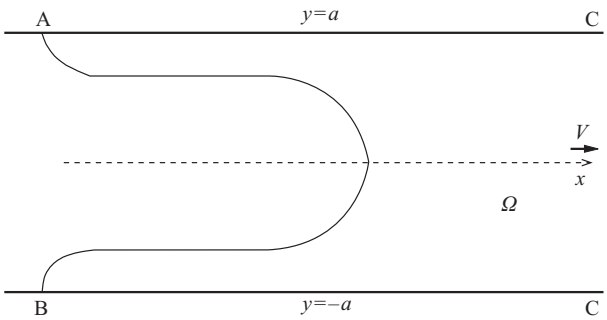

FIGURE 4. Hele-Shaw interface in the lateral plane in a channel geometry.

Hele-Shaw (1898) recognized that if low-Reynolds-number plane Poiseuille flow is averaged in the narrow gap direction, then the averaged velocity (u, v) in the (x, y)-plane satisfies the relation

$$(u, v) = -\frac{b^2}{12\mu}\nabla p \tag{1}$$

where p is the pressure, which is two-dimensional. Using incompressibility, it follows that

$$\nabla^2 p = 0. \tag{2}$$

The relations (1) and (2) are also satisfied by a Darcian flow in a porous medium with constant permeability (see Saffman & Taylor 1958), provided the constant $b^2T/12\mu$ in (1) is replaced by the permeability constant. At the interface between the two fluids of a Hele-Shaw interface (see figure 4), there is a pressure jump Δp due to surface tension effects, given by

$$\Delta p = \frac{2T}{b}\cos\chi + \frac{T}{R} \tag{3}$$

where χ is the contact angle (see figure 3) at the gap walls, which for simplicity is assumed to be a constant† at different points of the lateral interface (in figure 4). Since the viscosity of the less viscous fluid is ignored, it follows from (1) that regardless of the flow in the domain occupied by the less viscous fluid, $\nabla p = 0$; i.e. pressure is some constant p_0. Without any loss of generality $p_0 = 2T/b\cos\chi$ and so (3) reduces to

$$p = -\frac{T}{R}. \tag{4}$$

† Even in cases where there is no film, the contact angle χ actually depends on the normal component of fluid velocity. Such variations are accounted for by Weinstein, Dussan V. & Ungar (1990).

Also, the normal speed U_n of the interface is the same as the normal fluid velocity, i.e.

$$U_n = (u, v) \cdot \boldsymbol{n} \tag{5}$$

where $\boldsymbol{n}$ denotes unit interfacial normal vector. The interfacial conditions (4) and (5) have to be augmented by condition

$$v = 0 \tag{6}$$

on the sidewalls at $y = \pm a$, and asymptotic far-field conditions at ∞:

$$(u, v) = V\hat{\boldsymbol{x}} + o(1) \tag{7}$$

where $\hat{\boldsymbol{x}}$ is a unit vector in the positive x-direction.

We non-dimensionalize all lengths by the channel half-width a, and non-dimensionalize velocities by V, the displacement rate at ∞. Then, the non-dimensional velocity potential ϕ (which is proportional to the pressure) satisfies

$$\nabla^2\phi = 0 \quad \text{in flow domain } \Omega, \tag{8}$$

while on the interface

$$\phi = \frac{\mathscr{B}}{R} \tag{9}$$

and

$$\frac{\partial\phi}{\partial n} = U_n \tag{10}$$

where

$$\mathscr{B} = \frac{b^2 T}{12\mu V a^2} = \frac{\epsilon^2}{3Ca}; \tag{11}$$

the gap-width to cell-width ratio ϵ and capillary number Ca are as defined in § 2. At the sidewalls $y = \pm 1$,

$$\frac{\partial\phi}{\partial y} = 0 \tag{12}$$

and at $+\infty$,

$$\phi \sim x + O(1). \tag{13}$$

Equation (8) with interfacial conditions (9) and (10), boundary condition (12) and asymptotic far-field condition (13) determine ϕ and the location of the interface, generally characterized by a relation of the type $F(x, y, t) = 0$. We refer to these equations as McLean–Saffman (MS) equations. These have been widely used in the literature. The MS equations involve only one non-dimensional parameter $\mathscr{B}$ that lumps together cell-width to gap-width ratio ϵ and the capillary number Ca. Variations of this model were studied by introducing $\mathscr{B}$ that changes from point to point in some prescribed manner. As described later, these were meant to model localized effects of a small bubble in front of a finger, an interface-piercing-needle, or etched narrow-gap walls. Such variations are usually characterized by an additional parameter.

It is interesting to note that the MS equations of this section are close to those in a one-sided model of two-dimensional dendritic crystal growth, except that there are usually no sidewalls. Heat diffusion in the solid phase is neglected (see e.g. Misbah 1987). The non-dimensional temperature acts like the potential ϕ, where (9) and (10) are statements about lowering of melting temperature by the Gibbs–Thompson

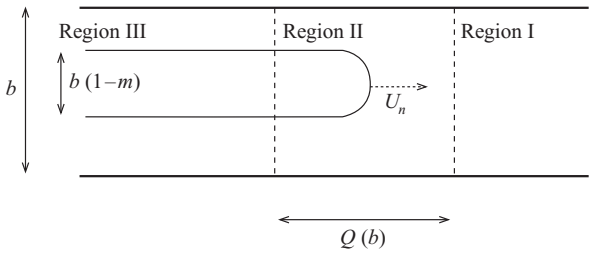

FIGURE 5. Thin-film next to the walls shown in the narrow-gap plane. Correspondences of regions I, II and III to the lateral flow domain shown in figure 6.

effect and the latent heat generated by the solidifying front as it advances into the undercooled fluid. Anisotropy in surface energy is usually modelled by letting $\mathscr{B}$ vary in some prescribed manner, similar to modelling anisotropic Hele-Shaw flow (Ben-Jacob *et al.* 1985). However, the Laplace equation (2) used for Hele-Shaw flow is only appropriate for the temperature in the small Péclet number (large diffusivity) limit, though not uniformly in the far field. Also, the far-field condition (13) is replaced by

$$\phi \sim -\Delta \tag{14}$$

for some specified undercooling Δ at ∞.

Chuoke *et al.* (1959) and Saffman & Taylor (1958) studied the linear stability of a planar front in a rectilinear geometry to find that it was unstable with growth rate

$$\sigma = |k|(1 - \mathscr{B}k^2) \tag{15}$$

where k is the wavenumber of the disturbance. Similar results were obtained for planar solidification fronts by Mullins & Sererka (1963), which in a limiting case reduces to (15).

The examination of the $\mathscr{B} \to 0$ limit is natural since many Hele-Shaw experiments do involve reasonably small $\mathscr{B}$. By setting $\mathscr{B} = 0$ in (9), we arrive at a simpler equation because of the absence of the $1/R$ term. Henceforth, with this simplification, the resulting MS equations will be referred to as the *idealized* equations. In the context of flow through a porous medium, these equations were used by Russian researchers in the mid forties (Galin 1945; Polubarinova-Kochina 1945). Ivantsov (1948) considered essentially the same idealized equation, though with finite diffusion effects, to determine a steadily advancing parabolic solidification front growing into an undercooled melt. Zhuravlev (1956) and Saffman & Taylor (1958) used the idealized equations in the theoretical calculations of a steady translating finger. Recently, in the problems of a heated plume rising in a Hele-Shaw cell (Ben Amar 1992) and filtration combustion (Aldusin & Matkowsky 1998), despite differences in physics, the same idealized equations have been arrived at, though in these cases surface tension is not appropriate.

In the next section, we discuss effective two-dimensional interfacial boundary conditions for Hele-Shaw flow that account for complications due to thin films adjacent to the gap walls. We will see that for some parameter ranges, these physically realistic boundary conditions do reduce to the MS boundary conditions. In some regimes, these equations approach the idealized equations, at least formally.

4. Thin-film complications

Generally, a thin film of the more viscous fluid is left behind next to the gap walls when the less viscous fluid advances (figure 5). Unlike the situation shown

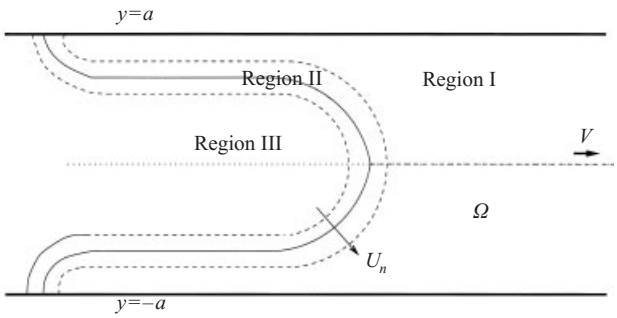

FIGURE 6. Flow domain in the lateral plane broken up into regions I, II and III.

in figure 3, the interface is not in contact with the gap walls. As in the last section, we ignore viscosity of the less viscous fluid and gravity effects in the present discussion.

Saffman (1982) discussed the possible form of the boundary conditions when thin-film effects are included. Following Bretherton's (1961) analysis of the motion of a bubble in a tube, Park & Homsy (1985) found concrete expressions for film thickness and pressure drops for small capillary number, Ca, while Reinelt (1987*a*, *b*) completed the asymptotic calculation of the $O(\epsilon)$ correction and the numerical calculations for $Ca = O(1)$. The presentation in this section follows Reinelt (1987*a*, *b*).

The flow domain, as viewed in the lateral plane, can be broken up into three regions, regions I, II and III as shown in figure 6. Regions I and III are far from the interface edge, in units of b. The fluid flow in regions I and III is modelled as a two-dimensional problem by averaging the Stokes flow across the thin film and narrow gap respectively. The averaged fluid velocity in the laboratory frame is proportional to the gradient of a pressure field p; in particular in region I, the gap-averaged velocity is given by the relation (1). The constant of proportionality between (u, v) and ∇p is different in the thin-film region III than in region I. The incompressibility condition translates into (2) in each of regions I and III.

In region II, whose width is $O(b)$, the three-dimensionality of the flow field is important. However, in the Hele-Shaw limit $b/a \to 0$, one can solve the region II equations to determine the asymptotic film thickness, m, relative to the gap width as well as determine pressure difference $\Delta p = p_I - p_{III}$ between regions I and III, as region II is approached, as a function of the normal interfacial velocity U_n and curvature $1/R$ of the interface edge in the lateral plane (figure 6).

These provide the boundary conditions in the (x, y)-plane linking flow regions I and III. These boundary conditions are then applied at the leading edge of the interface, since region II is of negligible thickness compared to the lateral length scale a. It is shown that

$$\Delta p = \frac{2T}{b}\left[\kappa^0(\mu U_n/T) + \kappa^1(\mu U_n/T)\frac{b}{2R} + O(b^2/R^2)\right], \tag{16}$$

$$m = m^0(\mu U_n/T) + m^1(\mu U_n/T)\frac{b}{2R} + O(b^2/R^2). \tag{17}$$

The four functions m^0, m^1, κ^0 and κ^1 are in general determined numerically by solving region II equations (Reinelt 1987*a*). However, in the limit $Ca \to 0$, following Bretherton's (1961) analysis for the motion of a bubble in a tube, Park & Homsy

(1985) and Reinelt (1987*a*) find that

$$\kappa^0(Ca) = -1 - 3.878Ca^{2/3} + O(Ca), \tag{18}$$

$$\kappa^1(Ca) = -\pi/4 + 4.153Ca^{2/3} + O(Ca), \tag{19}$$

$$m^0(Ca) = 1.3375Ca^{2/3} + O(Ca), \tag{20}$$

$$m^1(Ca) = -1.3375\frac{\pi}{4}Ca^{2/3} + O(Ca). \tag{21}$$

It is to be noted that while the derivation of (16) and (17) assumed steady flow, they remain equally valid for the unsteady gap-averaged problem when the time scale of lateral plane interface motion is $O(a/V)$, which is far larger than b/V, the time scale associated with transverse film adjustment. To the leading order, the pressure field in the thin-film region next to the transverse walls (region III) is uniform (zero without loss of generality), and consequently fluid flow can be ignored there (in the laboratory frame). This leads to a free boundary problem involving region I alone, where pressure p satisfies Laplace's equation (2), and at the interface (16) approximately reduces to:

$$p = \frac{2T}{b}\left[\kappa^0(\mu U_n/T) + \kappa^1(\mu U_n/T)\frac{b}{2R}\right]. \tag{22}$$

Using continuity of fluid flux between regions I and III,

$$\bar{u}_n = U_n[1 - m] \tag{23}$$

where $\bar{u}_n$ is the normal component of fluid velocity, and U_n is the normal interface velocity (both in the laboratory frame). If we introduce velocity potential ϕ (which is harmonic) and non-dimensionalize as in § 3, the interfacial boundary conditions (22) and (23) at the free boundary $F(x, y, t) = 0$ become

$$\phi = -\frac{\epsilon}{3Ca}\left[\kappa^0(\mu U_n/T) + \kappa^1(\mu U_n/T)\frac{\epsilon}{R}\right], \tag{24}$$

$$\frac{\partial\phi}{\partial n} = U_n(1 - m), \tag{25}$$

where the asymptotic relative thickness of thin film is given by

$$m = m^0(\mu U_n/T) + \frac{\epsilon}{R}m^1(\mu U_n/T). \tag{26}$$

Equation (8) in the domain Ω (figure 6), together with boundary conditions (12) on the channel walls, far-field conditions (13) and the interfacial conditions (24) and (25) completely determine ϕ and the interfacial boundary.† We will refer to these as the Saffman–Park–Homsy–Reinelt (SPHR) equations, because of the contributions of each investigator in the development.

It is to be noted that there are two distinct parameters in this problem: the gap-width to cell-width ratio ϵ and the capillary number $Ca = \mu V/T$. When $Ca \ll 1$, the approximations (18)–(21) are valid. Ignoring the constant term in the expansion of κ^0, which can be absorbed into ϕ without any loss of generality, we note that the SPHR equations (24)–(25) formally reduce to the idealized problem of the last section when $\epsilon Ca^{-1/3} \ll 1$ and $\epsilon^2/Ca \ll 1$. However, as is the case for the lateral curvature term in the MS equations for small $\mathscr{B}$, small SPHR corrections to the idealized

† SPHR interfacial conditions only hold for an advancing interface. For a receding interface, as in the rear of a translating bubble, additional complications arise (see Burgess & Foster 1990).

equation are fundamentally important, despite their apparent smallness. We also note from (18)–(21) that the more general MS equations of § 3 (with a $\pi/4$ multiplicative correction in $\mathscr{B}$) are recovered when $\epsilon^2/Ca \gg \epsilon Ca^{-1/3}$, i.e. $\epsilon \gg Ca^{2/3}$. Further, by applying (18)–(19), we note that in the range $1 \gg Ca^{2/3} \gg \epsilon$, the variation of κ^0 with U_n in (24) is formally larger than the $\kappa^1\epsilon/R$ term. So, it might appear that the latter term should be dropped in this limit. Yet, this underestimates the importance of the κ^1 term, when $\epsilon^2/Ca \ll 1$. The reasons for this will be discussed in the next section.

The thin-film effects also alter the linear-stability relation (15) for a planar interface. It was determined (unpublished work by the present author with D. A. Reinelt and P. G. Saffman 1993) that the growth rate for an infinitesimal disturbances is given (for our choice of non-dimensionalization) by

$$\sigma = \left(|k| + \frac{\epsilon^2}{3Ca}|k|^3\kappa^1 + \frac{\epsilon k^2 m^1}{1-m^0}\right) \Big/ \left(1 - m^0 - \frac{Cam^{0'}}{1-m^0} - \frac{\epsilon|k|}{3}\kappa^{0'}\right). \tag{27}$$

We note that m^1, κ^0, κ^1 and the derivative $\kappa^{0'}$ are all negative, while m^0 and its derivatives are positive. It is clear from the asymptotic relations (18)–(21) that (27) does reduces to (15) in a restricted range of the parameter space, except for a correction of $\mathscr{B}$ by a factor of $\pi/4$. This derivation is self-consistent only if the smallest scale in the lateral plane, which corresponds to $k = O(\mathscr{B}^{-1/2})$, is still far larger than b. This is only the case for $Ca \ll 1$. Earlier, Schwartz (1986) had obtained a similar relation, though it does not include all the terms in (27). Maxworthy (1989) discusses an instability mechanism for $Ca \gg 1$; this is not present under the conditions where (27) apply.

5. Steady finger formulation and selection problem

With the MS boundary conditions for a steady state, the kinematic boundary condition (10) reduces to

$$\frac{\partial\phi}{\partial n} = U\cos\theta \tag{28}$$

where U is the velocity of advance of the steady semi-infinite finger relative to the fluid velocity at ∞ and θ is the angle between the interface normal and the positive x-axis. Integrating $\nabla^2\phi$ over the flow domain Ω and using (12) and (13), one finds the finger width λ to be related to U as follows:

$$\lambda = \frac{1}{U}. \tag{29}$$

In a frame moving with the steady finger (figure 2), the kinematic boundary condition (28) transforms, without any loss of generality, into

$$\psi = 0 \tag{30}$$

where ψ is the stream function, so that $W = \phi + \mathrm{i}\psi$ is an analytic function of $z = x + \mathrm{i}y$, while the pressure condition (9) in the moving frame translates into

$$\phi + \frac{1}{\lambda}x = \frac{\mathscr{B}}{R}. \tag{31}$$

On the side walls, (6) implies that

$$\psi = \pm\left[\frac{1}{\lambda} - 1\right] \quad \text{on } y = -1 \text{ and } y = 1 \text{ respectively} \tag{32}$$

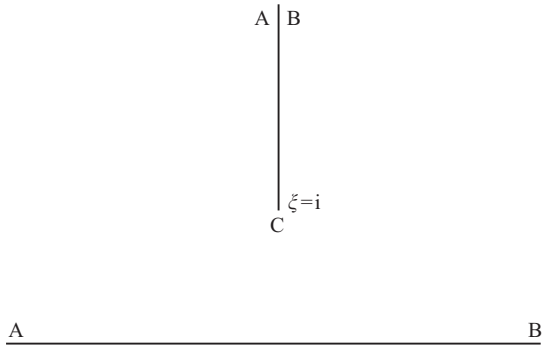

FIGURE 7. Upper half-ξ-plane, with a cut on the imaginary axis from $\xi = \mathrm{i}$ to $\mathrm{i}\infty$.

while the far-field conditions in the finger frame is

$$W \sim -\left[\frac{1}{\lambda} - 1\right] z + O(1). \tag{33}$$

Instead of formulating the problem in the z-domain, where the boundary is unknown *a priori*, it is common to consider the equivalent mathematical problem in a standard domain. There are a number of differing but equivalent formulations, starting with the one by McLean & Saffman (1981). Here, we use a variant of a more general formulation (Tanveer 1987*b*) that does not assume at the outset that the finger is symmetric about the channel centreline. The current formulation, like the one by McLean & Saffman (1981), is only suitable for a finger that is assumed *a priori* to be symmetric. Despite this restriction, we present this formulation because it is easier to understand the relevance of the illustrative example of § 6.

Consider the conformal map $z(\xi)$ of the cut upper half-ξ-plane, as shown in figure 7, to the flow domain outside the steady finger (figure 2). The two sides of the branch cut in figure 7 correspond to the two sidewalls, with the left- and right-hand sides of the cut corresponding to upper and lower walls, respectively. Further, the real ξ-axis corresponds to the finger boundary, with $\xi = -\infty, +\infty$ corresponding to the finger tails at $z = -\infty + \mathrm{i}\lambda$ and $z = -\infty - \mathrm{i}\lambda$, respectively. Correspondence of the three boundary points uniquely determines this conformal map. It is easily seen that the complex potential $W(\xi)$ is given by

$$W(\xi) = \frac{1-\lambda}{\pi\lambda} \ln(\xi^2 + 1) + \phi_0, \tag{34}$$

where ϕ_0 is some real constant. It is seen that (34) satisfies streamline condition $\psi = \operatorname{Im} W = 0$ on the real ξ-axis as it must, while on the right- and left-hand sides of the cut, its imaginary part satisfies (32). Further, we define $F(\xi)$ so that

$$z(\xi) = -\frac{1}{\pi} \ln(\xi - i) - \frac{(1-2\lambda)}{\pi} \ln(\xi + \mathrm{i}) - \mathrm{i}\lambda - \frac{2-2\lambda}{\pi} F(\xi). \tag{35}$$

The condition $\operatorname{Im} z = \pm 1$ on the two sides of the cut in the ξ-plane implies from (35) that $\operatorname{Im} F = 0$ there. From the flow geometry and symmetry assumptions, at points on the two walls $y = \pm 1$ corresponding to the same x, the complex velocity $\mathrm{d}W/\mathrm{d}z$ is the same. This translates into the requirement that $F(\xi)$ is the same on the two sides of the cut, i.e. there is no cut for $F(\xi)$ in the upper-half ξ-plane. This means that $\xi = \mathrm{i}$ is not a singularity of F, since any such singularity will have to be a pole, which is impossible for the conformal map $z(\xi)$. It follows that $F(\xi)$ is analytic in the

entire upper-half ξ-plane. It is easily seen that the remaining pressure condition (31) translates, with suitable choice of ϕ_0, into requiring that on the real ξ-axis

$$\operatorname{Re} F = \frac{\delta}{|F' + H|} \operatorname{Im}\left[\frac{F'' + H'}{F' + H}\right] \tag{36}$$

where

$$H(\xi) = \frac{\xi - p}{\xi^2 + 1} \quad \text{with } p = -\mathrm{i}\frac{\lambda}{1-\lambda} \quad \text{and} \quad \delta = \frac{\pi^2 \lambda \mathscr{B}}{4(1-\lambda)^2}. \tag{37}$$

The relation (36), which holds for a symmetric finger, is essentially the same as that obtained before (Tanveer 1987*b*), except that the work domain is now an upper half-ξ-plane, rather than the interior of a unit semicircle in the ζ-plane.

In the current formulation, the problem of determining a steady finger is equivalent to determining analytic function F in the upper-half ξ-plane that asymptotes to zero algebraically at ∞ and satisfies boundary condition (36) on the real ξ-axis; also it is necessary that for such an F, $F' + H$ is non-zero everywhere in the upper half-plane (a necessary condition for the mapping $z(\xi)$ to be conformal). For $\mathscr{B} = 0$, i.e. $\delta = 0$, it follows from (36) that

$$F = 0. \tag{38}$$

This corresponds to the solution independently worked out by Zhuravlev (1956) (which appeared in the Russian literature, though unknown in the West until recently) and Saffman & Taylor (1958). We refer to this as Zhuravlev–Saffman–Taylor (ZST) solution. With $F = 0$, (35) gives a parametric representation of the interface in the form $(x(\xi), y(\xi))$, where ξ is real. On eliminating ξ, we arrive at the more explicit representation for the interface corresponding to the ZST solution:

$$x = 2\frac{1-\lambda}{\pi} \ln \cos\left(\frac{\pi y}{2\lambda}\right). \tag{39}$$

The parameter λ (the relative finger width) remains arbitrary, in conflict with the experimental results of Saffman & Taylor (1958). There, λ was close to one half, except at small displacement rates V (when $\mathscr{B}$ is not small). This is not the only degeneracy when $\mathscr{B} = 0$. Taylor & Saffman (1959) obtained non-symmetric finger solutions, that allowed the distance β of the finger tip from the channel centreline as well as finger width λ to be arbitrary. Yet, experimental observations show that under normal conditions only a symmetric finger is observed. Here, we concentrate on the λ degeneracy of symmetric fingers. Similar degeneracy of solutions occur at $\mathscr{B} = 0$ for a steadily translating symmetric bubble of given area (Taylor & Saffman 1959). The bubble speed U relative to fluid displacement at ∞, as well as its location β relative to the channel centreline, remain arbitrary when $\mathscr{B} = 0$. Within the more general class of solutions where bubbles are not symmetric about the channel centreline, the degeneracy is again two-fold for given area (Tanveer 1987*a*). Also, there is a degenerate family of steadily travelling parabolic needle crystals in an undercooled liquid (Ivantsov 1948). Only the product of tip velocity and tip radius is determined as a function of undercooling and material properties; yet, experimentally each of the tip velocity and tip radius appear to be well determined (Huang & Glicksman 1981). In the latter case, unlike Hele-Shaw flow, there is no intrinsic length scale in the absence of surface energy, and so the degeneracy is not unexpected.

The disagreement between the idealized theory and the Saffman–Taylor experiment had been a puzzling riddle for many years. Based on Saffman–Taylor (1958) exper-

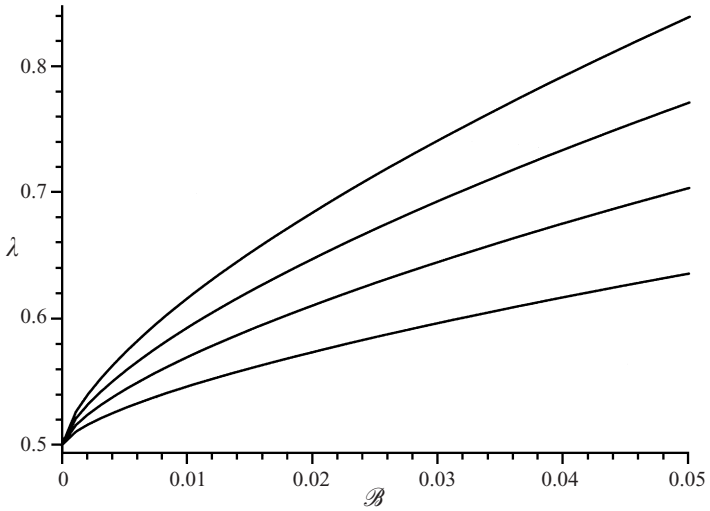

FIGURE 8. Sketch of λ vs. $\mathscr{B}$ dependence for the MS boundary conditions (Vanden-Broeck 1983).

imental conditions, one can estimate the size of each of the neglected terms in the SPHR boundary conditions. These terms are indeed found to be small, at least over the class of finger shapes which match experiment. What remained most puzzling is why, despite good agreement with a particular subset of solutions, other ZST shapes were not experimentally observable, though one can go through steps 1–3 in the introduction. Taylor & Saffman (1959) found that the $U = 2$ bubble solution can be distinguished by invoking some extremal principle. In the limit of large bubble size, the bubble front corresponds to the $\lambda = \frac{1}{2}$ finger solution, however, as noted by Saffman (1986), these distinguishing features of the $\lambda = \frac{1}{2}$ solution appeared to have no particular physical significance. In explaining selection of steady fingers arising in the context of filtration combustion, where surface tension is not appropriate, Aldushin & Matkowsky (1999) invoked similar arguments to describe selection of the $\lambda = \frac{1}{2}$ ZST solution. The linear stability analysis (Saffman & Taylor 1959) also gave puzzling results since it suggests that the solutions were unstable for any λ. So the stability calculation not only failed to give a criterion for selection, it also disagreed with experiments in which ZST shapes were observed.

For the MS equations, McLean & Saffman (1981) carried out a numerical calculation for non-zero $\mathscr{B}$. Their numerics suggested that for non-zero surface tension, λ was not arbitrary, but was some function $\lambda = \lambda(\mathscr{B})$, which approached $\frac{1}{2}$ as $\mathscr{B} \to 0^+$. Later, Romero (1982) and Vanden-Broeck (1983) determined a discrete family of steady branches of steady solutions for which $\lambda = \lambda_n(\mathscr{B})$, where n is an integer denoting the branch, with n increasing for increasing λ (figure 8). For fixed n, the λ corresponding to any of these solutions approached $\frac{1}{2}$. The numerical calculations of Kessler & Levine (1986*a*, *b*, 1987) suggested that only one branch was stable, while others were unstable, explaining why one branch appears to be experimentally observable.† Based on their numerics, Kessler & Levine (1986*a*, *b*) also suggested that there is a discontinuity in the spectrum at $\mathscr{B} = 0$. In particular, the Saffman & Taylor (1959) modes of instability were not part of the limiting spectrum as $\mathscr{B} \to 0^+$.

† Earlier numerical calculations of stability by McLean & Saffman are known to be in error due to an oversight pointed out by Sarkar (1985, private communication).

However, the steady calculation of McLean & Saffman (1981) was not conclusive at the time since there was a disagreement between their numerical calculations and asymptotics involving powers of $\mathscr{B}$. The latter failed to produce any restriction on λ. In our present formulation, the McLean–Saffman expansion is equivalent to

$$F \sim \delta F_1 + \delta^2 F_2 + \cdots. \tag{40}$$

From (36) and Poisson's integral formula, it is clear that for $\operatorname{Im}\xi > 0$,

$$F_1(\xi) = \frac{1}{\pi \mathrm{i}} \int_{-\infty}^{\infty} \frac{\mathrm{d}\xi'}{\xi' - \xi} \frac{1}{|H|} \operatorname{Im}\left[\frac{H'}{H}\right](\xi'). \tag{41}$$

In a recursive manner, $F_n(\xi)$ can be computed without any restriction on λ. The assumed asymptotic expansion (40) is, however, invalid as $\xi \to \infty$ (corresponding to finger tail) and a secondary expansion is needed (McLean & Saffman 1981); however, this expansion can be matched to (40) to at least four terms (McLean 1980), without any restriction on λ. The lack of selection through an asymptotic expansion of the form (40) is clearer in the closely related mathematical problem of a steady symmetric bubble (Tanveer 1986). Here, a series expansion in powers of $\mathscr{B}$ has been shown to be consistent to all orders in $\mathscr{B}$, without any restriction on bubble speed. Though there is no inconsistency in the asymptotic expansion (40) in the physical domain, for later reference it is important to note that it does become invalid at the complex turning point $\xi = p$. This is in the lower-half complex-plane and therefore does not correspond to any part of the actual flow domain. To see the disordering of the asymptotic expansion, it is necessary to analytically continue (36) to the lower-half complex-plane. For that purpose, it is convenient to define function $\bar{G}$, associated with G, as

$$\bar{G}(\xi) = [G(\xi^*)]^*. \tag{42}$$

Here, the superscript $*$ denotes complex conjugation. It is clear that $\bar{G}$ is an analytic function at ξ in the lower-half plane, when the corresponding G is analytic in the upper half-plane at ξ^*. In particular, it follows that

$$\bar{H}(\xi) = \frac{\xi + p}{\xi^2 + 1}.$$

Also, if F is analytic everywhere in the upper half-plane, $\bar{F}$ will be analytic everwhere in the lower half-plane. For analytic continuation purposes, it is convenient to notice that on the real axis

$$\frac{1}{|F' + H|} \operatorname{Im}\left[\frac{F'' + H'}{F' + H}\right] = \frac{1}{2\mathrm{i}(F' + H)^{1/2}(\bar{F}' + \bar{H})^{1/2}} \left[\frac{F'' + H'}{F' + H} - \frac{\bar{F}'' + \bar{H}'}{\bar{F}' + \bar{H}}\right]. \tag{43}$$

By using Poisson's integral formula on (36), it is clear that the upper half-ξ-plane

$$F(\xi) = \frac{\delta}{\pi \mathrm{i}} \int_{-\infty}^{\infty} \frac{\mathrm{d}\xi'}{\xi' - \xi} \frac{1}{|F' + H|} \operatorname{Im}\left[\frac{F'' + H'}{F' + H}\right](\xi') \equiv \delta I(\xi). \tag{44}$$

Through a standard process of contour deformation, the analytic continuation of (44) gives rise to the following integro-differential equation in the lower-half complex-ξ-plane:

$$F(\xi) = \delta I(\xi) + \frac{\delta}{\mathrm{i}(F' + H)^{1/2}(\bar{F}' + \bar{H})^{1/2}} \left[\frac{F'' + H'}{F' + H} - \frac{\bar{F}'' + \bar{H}'}{\bar{F}' + \bar{H}}\right](\xi) \tag{45}$$

where $I(\xi)$ is the analytic function defined by the same expression as on the right-

hand side of (44), except that ξ is in the lower half-plane. In particular, the analytic continuation reveals that the leading-order term F_1 satisfies

$$F_1(\xi) = I_1(\xi) + \frac{1}{\mathrm{i}H^{1/2}\bar{H}^{1/2}}\left[\frac{H'}{H} - \frac{\bar{H}'}{\bar{H}}\right](\xi) \tag{46}$$

where $I_1(\xi)$ is the same as I, when $F = 0$ is substituted into it. From the expressions for H and $\bar{H}$ and the analyticity of $I_1(\xi)$ in the lower half-plane, it follows that $F_1(\xi)$ is indeed singular at $\xi = p$, where $H = 0$. Substituting the asymptotic expansion (40) into the integro-differential equation (45), it is not difficult to see that the singularities of $F_2(\xi)$, $F_3(\xi), \ldots$ are progressively worse at the turning point $\xi = p$ in the lower-half complex-plane. This turning point plays a crucial role in determining exponentially small corrections to the asymptotic series (40) and these need to be accounted for in determining λ. This process will be explained in the illustrative example of the next section.

Following intuition gained from simple models of crystal growth, Kessler & Levine (1985) were the first to suggest that exponentially small terms missing in the McLean–Saffman perturbation expansion were the reason for the discrepancy with numerical calculations. Their numerical calculations supported this contention. This was later confirmed both for fingers and bubbles through an asymptotic procedure that extracted the leading-order exponentially small term in δ (Combescot *et al.* 1986, 1987; Hong & Langer 1986; Shraiman 1986; Tanveer 1986, 1987*b*; Dorsey & Martin 1987; Combescot & Dombre 1988). Though not all the different procedures are entirely correct, they do give rise to the same results in a qualitative sense. Nonlinearity, as first included by Combescot *et al.* (1986), is found to be important (Tanveer 1987*b*; Dorsey & Martin 1987; Combescot *et al.* 1987) in determining the correct scaling constants.

Indeed, taking account of exponentially small terms (Tanveer 1987*c*) is also crucial in determining the linear stability spectrum. As $\mathscr{B} \to 0$, the limiting spectrum is different from that at $\mathscr{B} = 0$. Different branches of solution (see figure 8) can have differing stability properties, even as they approach the same ($\lambda = \frac{1}{2}$) ZST solution. These results are, however, inconsistent with a linear stability calculation procedure (Xu 1991) that in effect ignores surface tension corrections in the underlying steady-state solution. Otherwise all the branches shown in figure 8 would have the same stability features asymptotically as $\mathscr{B} \to 0^+$. Also, a corollary that follows from the merging of linearly unstable and stable branches is that the threshold amplitude for nonlinear instability must shrink to zero as $\mathscr{B} \to 0^+$. This was realized by Bensimon (1986), and explains why steady fingers are not observed in experiment when $\mathscr{B}$ is too small. The numerical simulation of an unsteady finger by DeGregoria & Schwartz (1986) shows sensitive dependence of tip splitting on noise, in conformity with the above.

Numerical (Ben-Jacob *et al.* 1985; Zocchi *et al.* 1987) and formal asymptotic calculations (Kessler, Koplik & Levine 1986; Dorsey & Martin 1987; Ben Amar, Combescot & Couder 1993; Shaw 1989; Hong & Family 1988) also suggest that if surface tension is varied near the finger tip, so as to model tip perturbations due to a bubble, needle or etched gap walls, then it is possible to obtain a limiting ZST (or Taylor–Saffman) solution where λ differs significantly from 1/2 or the finger is not symmetric.

Numerical calculations of steady fingers using SPHR equations of Reinelt (1987*b*) gave a more accurate comparison with theory and in particular showed that it was

possible to get limiting solutions for small $\mathscr{B}$ that approach a ZST solution with λ somewhat less than $\frac{1}{2}$, in conformity with experiment. Reinelt's calculations specifically showed that the leakage term m, though formally estimated to be small and neglected in earlier calculations of Schwartz & DeGregoria (1987) and Sarkar & Jasnow (1987), is crucial in getting the finger width $\lambda < \frac{1}{2}$ for small $\mathscr{B}$. Tanveer (1990) used a formal asymptotic calculation to confirm the results of Reinelt in the limiting cases, as well as show that in the range $\epsilon \ll Ca \ll 1$, the leakage term m^0 plays a vital role in determining λ, which is obtained from the relation

$$\frac{\lambda^2(1-\lambda)}{(1-2\lambda)} = k_n \frac{\epsilon}{Ca^{3/2}} \tag{47}$$

where the k_n are a discrete set of positive constants, characteristic of the branch of solution, with only the smallest k_n corresponding to a linearly stable solution (Tanveer 1996). In particular, (47) implies that if experiment were carried out with $\epsilon = O(Ca^{3/2})$, with $Ca \ll 1$, then, one can access ZST solutions with λ significantly less than $\frac{1}{2}$.†

All the above results suggest clearly that the solution selected in the limit as some physical regularization tends to zero depend sensitively on the nature of correction (either constant surface tension, variable surface tension or thin-film corrections). This sensitive dependence on the nature of regularization to the idealized problem is not consistent with explanations (Mineev-Weinstein 1998) of finger width selection based on the idealized solutions themselves. For the same reason, a uniform extremum principle to explain steady-state selection (Aldusin & Matkowsky 1999), independent of the nature of regularization, appears to be unsatisfactory. An important point here is that the correction to the idealized equation need not be restricted to surface-tension-type terms. In some physical problems, surface tension may not even be appropriate. One can expect that the particular ZST solution selected depends in general on the nature of the correction involved.

The results for steady needle crystals in two-dimensions are a bit different. At least, within the class of solutions that approach a parabolic shape in the far field, numerical (Meiron 1986; Kessler *et al.* 1986) as well as analytic investigations (Barbeiri, Hong & Langer 1986; Ben Amar & Pomeau 1986; Misbah 1987; Ben Amar 1988; Tanveer 1989) show that no solutions exist for constant surface tension. However, for a model with anisotropic surface tension, a discrete set of steady solutions is possible, only one of which is linearly stable (Kessler & Levine 1986*a*, *b*; Brener & Melnikov 1990). The tip radius of the theoretically selected solution, however, diverged as anisotropy tends to zero. Such strong dependences in the limit are apparently not consistent with experimental observations for Pivalic acid (Glicksman & Marsh 1993).

We summarize some of the seemingly surprising features of the steady-state fingers that have emerged to date:

1. For any $\lambda \in (0,1)$ small curvature terms play a singular role, even though it would seem otherwise based on steps 1–3 of the introduction. The solution set for $\mathscr{B} = 0$ is indeed different from that as $\mathscr{B} \to 0^+$. These results demonstrate the structural instability of the idealized problem.

2. When the MS equations are altered, either by varying surface tension or introducing SPHR thin-film corrections, it is possible to select fingers from the ZST family or even the Taylor–Saffman family that are different from the $(\lambda, \beta) = (\frac{1}{2}, 0)$ solution.

3. The spectrum is discontinuous at $\mathscr{B} = 0$. As for steady-state selection, only

† Small ϵ gives rise to large pressure variations that can bend the gap plates in an experiment.

particular $\mathscr{B} = 0$ modes are selected as $\mathscr{B} \to 0^+$. This is seen explicitly for small Hele-Shaw bubbles (Tanveer & Saffman 1987). Also, the spectrum for different branches of solution is different, though all branches tend to the same ZST solution (figure 8).

4. When multiple small effects are present, such as the SPHR terms κ^0, κ^1, m^0 and m^1 for small $\mathscr{B}$ and small Ca, their relative importance is not always determined by their sizes in the physical domain. Rather, what matters is the size near a complex turning point and whether the inclusion of such a term stabilizes the resulting system structurally. This explains the apparently disproportional influence of the small leakage term m^0 for small $\mathscr{B}$, even for $Ca^{2/3} \gg \epsilon \gg Ca$ when (17)–(21), (24)–(26) imply that the variation of κ^0 is formally much larger than the leakage term m^0. It also explains why the $\epsilon\kappa^1/R$ term in (24) cannot be dropped altogether, even when it appears small. The latter is consistent with Romero's (1982) numerics that revealed no selection of λ in the absence of a lateral curvature term in the pressure equation.

In the following section, through a relatively simple example, we explicitly demonstrate how the above features can arise when we approach a point in the parameter space that corresponds to a structurally unstable system. Though this problem is contrived and has no direct relationship with Hele-Shaw fingers, it does illustrate many of the features of steady viscous fingering or the steady needle crystal problem. Further, as will be explained, the mathematics involved is not unrelated either.

6. Illustrative steady-state example

Consider the solution $\phi(x, y)$ to the following:

PROBLEM 1. *Solve*

$$\nabla^2\phi = 0 \tag{48}$$

in the upper half-plane domain $y > 0$ *satisfying the following condition:* ϕ *and all its derivatives are continuous as* $y \to 0^+$ *for any* x. *On the boundary of the domain,*

$$\epsilon\phi_{xxx}(x,0) + (1 - x^2 + a)\phi_x(x,0) - 2x\phi_y(x,0) = 1 \tag{49}$$

where $\epsilon > 0$ *and* a *is real in the interval* $(-1, \infty)$. *As* $x^2 + y^2 \to \infty$, $(x^2 + y^2)|\nabla\phi|$ *is bounded for* $y > 0$ *and higher derivatives of* ϕ *all vanish.*

We introduce a complex function $W(x + \mathrm{i}y) = \phi_x(x, y) - \mathrm{i}\phi_y(x, y)$. It is clear that $W(z)$ is an analytic function in the upper half-z-plane. The boundary condition (49) implies

$$\mathrm{Re}\,\{\epsilon W'' + [(1 - \mathrm{i}z)^2 + a]W - 1\} = 0$$

on the real z-axis. Clearly the quantity $\{\cdot\cdot\}$ is analytic in the upper half-plane and by Schwarz reflection an entire function. Further, from problem 1, it is clear that this quantity is also bounded. So, from Liouville's theorem, without any loss of generality†

$$\epsilon W'' + [(1 - \mathrm{i}z)^2 + a]W = 1. \tag{50}$$

It is clear that the question of existence of a solution to problem 1 is equivalent to whether the following problem has a solution or not:

PROBLEM 2. *Find an analytic function* $W(z)$ *satisfying* (50) *in* $\mathrm{Im}\,z > 0$ *with*

$$W(z) \to 0 \text{ as } z \to \infty \quad \text{for } \mathrm{Arg}\,z \in (0, \pi). \tag{51}$$

† Generally, we have a complex number $1 + \mathrm{i}c$ on the right-hand side of (50); however the corresponding solution is only different by a multiplicative factor.

We note that for $\epsilon = 0$, $W = W_0(z)$, where

$$W_0 = [(1 - \mathrm{i}z)^2 + a]^{-1}. \tag{52}$$

This is singular at $z = \pm\sqrt{a} - \mathrm{i}$, only in the lower-half complex-z-plane. Further, a formal asymptotic expansion can be constructed in powers of ϵ for $\epsilon \ll 1$:

$$W \sim W_0 + \epsilon W_1 + \cdots \tag{53}$$

with W_n for $n \geqslant 1$ determined recursively from

$$W_n = -[(1 - \mathrm{i}z)^2 + a]^{-1} W''_{n-1}(z). \tag{54}$$

It is clear that the asymptotic expansion (53) is consistent at all orders in ϵ for $\mathrm{Im}\, z \geqslant 0$. This is true for any a. The assumed expansion (53) is inconsistent only when $z = \pm\sqrt{a} - \mathrm{i}$ is approached in the lower half-plane, which is outside the original domain of interest. Thus, based on the formal validity of the asymptotic expansion (53) in the upper half-z-plane, one is tempted to conclude that Problem 2 (and therefore Problem 1) has a solution, at least for sufficiently small ϵ. It will be shown explicitly that this conclusion is incorrect because of the presence of terms that are exponentially small in ϵ for small ϵ. Indeed, it will be shown that a unique solution to Problem 2 exists if and only if the parameter a satisfies the 'quantum' condition:

$$a = 2\left(2n + \tfrac{3}{2}\right)\epsilon^{1/2} \quad \text{for integer } n \geqslant 0. \tag{55}$$

For convenience, we introduce scaled variables:

$$1 - \mathrm{i}z = 2^{-1/2}\epsilon^{1/4} Z; \quad W = 2^{-1}\epsilon^{-1/2} G(Z); \quad a = 2\epsilon^{1/2}\alpha. \tag{56}$$

Note that ϵ need not be small and the relation (55) is exact. The scaling (56) is done merely for convenience of presentation. It is clear that with these scalings, (50) becomes

$$G'' - \left(\tfrac{1}{4}Z^2 + \alpha\right) G = -1. \tag{57}$$

Since (57) allows only analytic solutions, which in particular are analytic on the part of the Z-plane corresponding to $\mathrm{Im}\, z > 0$, it is clear that Problem 2 is equivalent to (note the 90° rotation involved in defining Z relative to z in (56))

Problem 3. *Find a solution G to* (57) *so that*

$$G(Z) \to 0 \text{ as } Z \to \infty \quad \text{for } \mathrm{Arg}\, Z \in (-\pi/2, \pi/2). \tag{58}$$

It is to be noted that the associated homogeneous equation has solutions $G_1(Z)$, $G_2(Z)$, $G_3(Z)$ (not an independent set) that are related to the parabolic cylinder function $U(\alpha, Z)$ (Abramowitz & Stegun 1972) by the relation

$$\left.\begin{aligned} G_1(Z) = U(\alpha, Z); \quad G_2(Z) = \mathrm{e}^{-\mathrm{i}\pi(\alpha/2 - 1/4)} U(-\alpha, \mathrm{i}Z); \\ G_3(Z) = \mathrm{e}^{\mathrm{i}\pi(\alpha/2 - 1/4)} U(-\alpha, -\mathrm{i}Z) \end{aligned}\right\} \tag{59}$$

Any two of these form an independent set of solutions that span the solution set to the homogenous equation. Indeed, the Wronskian $\mathscr{W}(G_1, G_2) = 1$ and $\mathscr{W}(G_1, G_3) = 1$. From the integral representation of $U(\alpha, Z)$ (see p. 688, 19.5.4, Abramowitz & Stegun 1972), one can derive

$$G_2(Z) - G_3(Z) = 2\mathrm{i}k G_1(Z), \quad \text{where } k = \frac{\Gamma(\alpha + \frac{1}{2})}{\sqrt{2\pi}} \cos(\pi\alpha). \tag{60}$$

Further, from the known asymptotics of $U(\alpha, Z)$, it follows that as $Z \to \infty$,

$$G_1(Z) \sim Z^{-\alpha-1/2} e^{-Z^2/4} \quad \text{for } \operatorname{Arg} Z \in (-3\pi/4, 3\pi/4), \tag{61}$$

$$G_2(Z) \sim Z^{\alpha-1/2} e^{Z^2/4} \quad \text{for } \operatorname{Arg} Z \in (-5\pi/4, \pi/4), \tag{62}$$

$$G_3(Z) \sim Z^{\alpha-1/2} e^{Z^2/4} \quad \text{for } \operatorname{Arg} Z \in (-\pi/4, 5\pi/4). \tag{63}$$

LEMMA 1. *There exists a unique solution to* (57) *satisfying*

$$G(Z) \to 0 \text{ as } Z \to \infty \quad \text{for } \operatorname{Arg} Z \in (-\pi/2, 0] \tag{64}$$

given by

$$G(Z) = G_p(Z) \equiv G_1(Z) \int_{-i\infty}^{Z} G_2(\xi)\, d\xi - G_2(Z) \int_{\infty}^{Z} G_1(\xi)\, d\xi. \tag{65}$$

It follows from variation of parameters that $G_p(Z)$ is indeed a solution to (57). In the Appendix, we complete the proof of lemma 1, by rigorously showing that $G_p(Z) = O(Z^{-2})$ as $Z \to \infty$ in the sector $\operatorname{Arg} Z \in (-\pi/2, 0]$. This can be seen to be reasonable from integration by parts on steepest descent contours, after accounting for the asymptotic behaviour (61)–(62). The uniqueness in lemma 1 is a simple consequence of the fact that $C_1 G_1(Z) + C_2 G_2(Z)$ does not go to zero as $Z \to \infty$, for $\operatorname{Arg} Z \in (-\pi/2, 0]$ for non-zero (C_1, C_2).

Similar arguments lead to the following lemma:

LEMMA 2. *There exists a unique solution to* (57) *satisfying*

$$G(Z) \to 0 \text{ as } Z \to \infty \quad \text{for } \operatorname{Arg} Z \in [0, \pi/2) \tag{66}$$

given by

$$G(Z) = \hat{G}_p(Z) \equiv G_1(Z) \int_{i\infty}^{Z} G_3(\xi)\, d\xi - G_3(Z) \int_{\infty}^{Z} G_1(\xi)\, d\xi. \tag{67}$$

In view of lemmas 1 and 2, it is clear that problem 3 will have a solution if and only if

$$\hat{G}_p(Z) = G_p(Z). \tag{68}$$

Using (60), it is seen from (65) and (67) that

$$G_p(Z) - \hat{G}_p(Z) = G_1(Z) A(\alpha) \tag{69}$$

where $A(\alpha)$ involves integrals of the parabolic cylinder function (see the Appendix). So condition (68) implies that $A(\alpha) = 0$. It is shown in the Appendix that $A(\alpha) = 0$ if and only if

$$\alpha = \alpha_n \equiv 2n + \tfrac{3}{2} \quad \text{for integer } n \geqslant 0 \tag{70}$$

and so the quantum condition (55) follows. Some comments are in order about the results and mathematics involved here, as they relate to a steady viscous finger.

1. When $0 < \epsilon \ll 1$, it is to be noted that for an arbitary a, and therefore $\alpha \neq \alpha_n$, the difference between the solution $W(z)$ corresponding to $G(Z) = G_p(Z)$ and that corresponding to $G(Z) = \hat{G}_p(Z)$ is exponentially small in ϵ at $z = 0$ or any point on the positive imaginary z-axis. This is seen by using relations (56), (61) and (69). Such a term is absent in the regular perturbation expansion (53). This lack of selection in a regular perturbation expansion is similar to that discussed in § 5 for a finger.

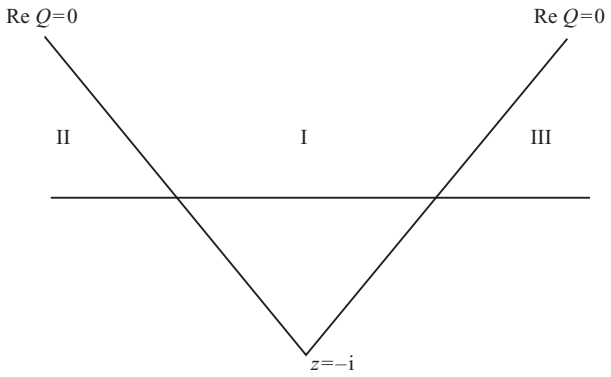

FIGURE 9. Stokes lines $\mathrm{Re}\, Q = \mathrm{Re}\, Q(-\mathrm{i})$ divide the upper half-plane into Stokes sectors I, II and III.

2. For any solution corresponding to $a = \alpha_n \epsilon$ for fixed n, as $\epsilon \to 0$, $a \to 0$ and $W \to W_0 = (1 - \mathrm{i}z)^{-2}$. For $a \neq 2\epsilon^{1/2}\alpha_n$, the corresponding W_0 in (52) is not the limiting solution as $\epsilon \to 0^+$. This is similar to the observation that with the MS equations, a ZST solution with $\lambda \neq \frac{1}{2}$ is not a limiting solution as $\mathscr{B} \to 0^+$ (except possibly for a non-constant $\mathscr{B}$). These features make the $\epsilon = 0$ structurally unstable, similar to the idealized problem discussed in § 5.

3. It is not crucial that the associated homogeneous equation (50) has closed form solutions. For small ϵ, WKBJ solutions suffice to obtain asymptotic answers for a. Equation (50) admits solutions of the form $\exp(\pm\epsilon^{-1/2}Q)$. After noting the change in variable (56), it is easy to see that the WKBJ solutions correspond to (61)–(62). What is important to the selection is that the anti-Stokes lines $\mathrm{Re}\, Q =$ constant emerging from $z = -\mathrm{i}$ segments the physical domain $\mathrm{Im}\, z \geqslant 0$ into three sectors, I, II and III (figure 9). Without conditions on a, it becomes impossible for a second-order differential equation to satisfy $W \to 0$ as $z \to \infty$ in all three sectors at the same time.

4. If the problem were nonlinear, similar arguments would hold except near turning points since the leading-order exponential terms in ϵ are determined from the homogeneous part of the linearized equation about a given zero-ϵ solution (Kruskal & Segur 1991). Nonlinearity can be important in determining the numerical value of a parameter like α in an inner equation near the turning point. For a problem involving only small parameter ϵ, nonlinearity does not change the scaling between a and ϵ, though it is important in determining the scaling constant. For problems involving multiple parameters, nonlinearity can be crucial (Tanveer 1990), as is the case in the derivation of (47).

5. For $\epsilon \ll 1$, it is not crucial that we were able to convert problem 1 into a differential equation for $W(z)$. Generally for boundary conditions more complicated than (49), as is the case in viscous fingering, the best that can be hoped for is an integro-differential equation (see (45) for instance). However, when the equation is analytically continued to a neighbourhood of a complex turning point(s) (marked by the breakdown of a regular perturbation expansion), the non-local integral terms (like $I(\xi)$, $\bar{F}(\xi)$ in (45) involve the unknown function on the real axis or in the upper half-plane). These terms are analytic at the turning points and do not play a crucial role.† They can be replaced by the corresponding values for $\epsilon = 0$ ($\mathscr{B} = 0$ for fingers). This simplification results in a differential equation in the complex plane, for which comment 4 above is applicable.

† See Xie (2000) for mathematically rigorous aspects of controlling non-local terms.

6. If additional small terms are added to equation (50), there can be dramatic effects on the solution set for small ϵ, even when such effects are estimated to be small in the physical domain compared to terms in (50). What matters is not the size of the terms in the physical domain but their sizes near relevant complex turning points.

Comment 6 is similar to comment 4 in § 5 about Hele-Shaw fingers. However, in the present model, we can illustrate this feature more easily by introducing the following variation of the model problem. Consider

$$\epsilon W'' + \left[(1-\mathrm{i}z)^2 + a + \frac{\epsilon_1}{(1-\mathrm{i}z)^2}\right] W = 1. \tag{71}$$

As before, we seek a solution so that $W(z) \to 0$ as $z \to \infty$, in the domain $\operatorname{Im} z > 0$. If we introduce the scaled variables as in (56), we obtain

$$G'' - \left(\tfrac{1}{4}Z^2 + \alpha + \frac{\gamma}{Z^2}\right) G(Z) = 1 \tag{72}$$

where

$$\gamma = \frac{\epsilon_1}{\epsilon}.$$

Clearly the problem for W stated above is equivalent to seeking a solution to (72) so that $G(Z) \to 0$, when $Z \to \infty$ for $\operatorname{Arg} Z \in (-\pi/2, \pi/2)$. The associated homogeneous equation (72) has solutions related to the Whittaker functions. Without going into details, we simply state that the solution exists if and only if

$$\alpha = \hat{\alpha}_n(\gamma).$$

When $\gamma \to 0$, $\hat{\alpha}_n \to \alpha_n = (2n + 3/2)$. The dependence on γ when γ is strictly order 1 (or larger) implies that we no longer have the previous scaling relation between a and ϵ. Instead, ϵ_1 enters into the relation. This change of scaling is possible even when $\epsilon \ll \epsilon_1 \ll \epsilon^{1/2}$, which is surprising. In that case, $\epsilon_1/(1-\mathrm{i}z)^2 \ll \epsilon^{1/2}$ in the upper half-z-plane and the real axis (domain of interest), and from (71) it might appear that any deviation from the previous result $a = 2(2n + 3/2)\epsilon^{1/2}$ should be small. This illustrates our comment (6) – that $\epsilon_1/(1-\mathrm{i}z)^2$ is important because of its size near the complex point $z = -\mathrm{i}$, even though it is outside the physical domain. We also note that even when ϵ_1 far exceeds ϵ, we cannot drop the latter, as otherwise there is no selection of a. On the other hand, the equations with $\epsilon \neq 0$ and fixed are structurally stable, unlike the system for $\epsilon = 0$. So, while the size of the terms near the turning points must be considered, it is also important to ascertain that the correction to the idealized equation structurally stabilizes the resulting system.

We also note that all sensitivity to the ϵ_1 term disappears as ϵ is made larger. If ϵ is not as small, ϵ_1 will have to be larger in order for γ to be strictly $O(1)$. Hence changes in the previous result $a = 2(2n + \frac{3}{2})\epsilon^{1/2}$ will indeed be small for small enough ϵ_1. Similarly, for the viscous fingering problem, if the surface tension parameter $\mathscr{B}$ is not that small, we do not get as much sensitivity, as born out in numerical calculations (McLean & Saffman 1982) and physical experiment.

7. Initial value problem

In this section, we will limit ourselves to discussions of the singular aspects of the initial value problem in the asymptotic limit $\mathscr{B} \to 0^+$. We will only consider the MS boundary conditions, though some aspects of the dynamics have been explored for SPHR equations as well (Tanveer 1996).

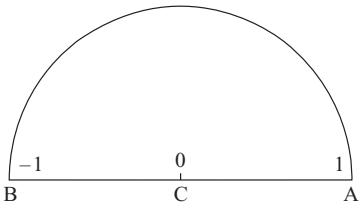

FIGURE 10. Unit upper half-semicircle in the ζ-plane.

There are a number of different formulations possible. The formulation described follows that in Tanveer (1993), which is close to the one used earlier by Bensimon (1986). Consider the conformal map $z(\zeta,t)$ that maps the interior of the unit semicircle in the ζ-plane (figure 10) to the physical domain (figure 4) with point correspondences as shown in the figures. At any finite time t, the points A and B are finite points, unlike the case of a steady finger. We can clearly decompose

$$z(\zeta,t) = -\frac{2}{\pi}\ln\zeta + \mathrm{i} + f(\zeta,t) \tag{73}$$

where $f(\zeta,t)$ is analytic inside the unit semicircle. Further, on the real axis between -1 and $+1$, the geometric condition that the sidewalls are at $\mathrm{Im}\, z = \pm 1$ corresponds to the requirement

$$\mathrm{Im}\, f = 0. \tag{74}$$

Since the singularity of $z(\zeta,t)$ at $\zeta = 0$ is incorporated in the log term in (73) such that f is continuous at $\zeta = 0$, it follows from the reflection principle that f is analytic for $|\zeta| < 1$. Further, for interfaces which are analytic, the finger is analytic on $|\zeta| = 1$ with the possible exception of $\zeta = \pm 1$. If the extended interface formed by reflection about each of the sidewalls is also assumed to be smooth, then analyticity follows at $\zeta = \pm 1$ as well. We decompose the complex velocity potential $W(\zeta,t)$ defined as $\phi + \mathrm{i}\psi$ as

$$W(\zeta,t) = -\frac{2}{\pi}\ln\zeta + \mathrm{i} + \omega(\zeta,t). \tag{75}$$

The fluid velocity at infinity is assumed to be unity without any loss of generality when the pressure gradient at infinity is time independent, as is assumed here. It is clear that the condition of no flow through the walls implies

$$\mathrm{Im}\,\omega = 0 \tag{76}$$

on the real diameter $(-1,1)$ of the unit semicircle. Further, ω is assumed to be continuous up to the real diameter including $\zeta = 0$, which is physically reasonable. It will also be assumed that ω is analytic on the semicircular arc corresponding to a smooth flow at the interface. From the Schwartz reflection principle, (76) implies that ω is analytic in $|\zeta| \leqslant 1$. The pressure boundary condition (9) on $|\zeta| = 1$ corresponds to

$$\mathrm{Re}\,\omega = -\frac{\mathscr{B}}{|z_\zeta|}\,\mathrm{Re}\left[1 + \zeta\frac{z_{\zeta\zeta}}{z_\zeta}\right]. \tag{77}$$

The kinematic condition given in (10) may be written as

$$\mathrm{Re}\left[\frac{\zeta W_\zeta}{|z_\zeta|^2} - \frac{z_t}{\zeta z_\zeta}\right] = 0. \tag{78}$$

Equations (77) and (78) determine the evolution of the functions f and ω as defined in (73) and (75). In the special case when $\mathscr{B} = 0$, it is clear from (77) that, without any loss of generality,

$$\omega = 0. \tag{79}$$

In that case, it follows from (75) and (78) that

$$\mathrm{Re}\left[\frac{z_t}{\zeta z_\zeta}\right] = -\frac{2}{\pi}\frac{1}{|z_\zeta|^2}. \tag{80}$$

Although this equation has been derived only for the channel geometry, a small change in the decomposition (73) (putting a simple pole rather than a log term) and working with the full ζ circle allows us to consider the radial geometry problem as well.

There is a very extensive body of literature (which we do not review here) for the $\mathscr{B} = 0$ problem, starting with exact solution methodologies appearing in the Russian literature by Galin (1945) and Polubarinova-Kochina (1945) (see Hohlov 1990 for a review of these works). Some of the later works in the West follow as applications of those methodologies, though they do not seem to have been noticed by researchers outside of Russia. The class of exact solutions is very rich and includes ones that evolve to a smooth finger (Saffman 1959; Howison 1985; Mineev-Weinstein & Ponce-Dawson 1994), or ones that form interfacial singularities (cusps) in a finite time (Shraiman & Bensimon 1984). Essentially, if z_ζ is initially any rational function, including f being a polynomial of arbitrary order, it is known that the corresponding rational function form is preserved in time. However, as originally noted by Howison (1986), the idealized initial value problem (i.e. $\mathscr{B} = 0$) is ill-posed, i.e. solutions at a given time do not have continuity with respect to variations in initial shape (with respect to any interface-based norm that is sensitive to the interface slope). Ill-posedness is also known to occur in the stronger sense of Hadamard (see for example discussions in Fokas & Tanveer 1998), meaning that the time needed for two solutions to diverge can be made arbitrarily small. Because of this ill-posedness, any particular solution to $\mathscr{B} = 0$ (idealized problem) need not be physically meaningful, since one does not have exact control over the initial shape in an experiment. Nonetheless, because of our ability to generate explicit solutions to the idealized problem, it is important to know if such a solution is the limiting solution to the initial value problem as $\mathscr{B} \to 0^+$. Unfortunately, however, the $\mathscr{B} \neq 0$ problem remains difficult to analyse. There is a mathematically rigorous proof only for the short-time existence of smooth solutions (Duchon & Robert 1984). However, there is no rigorous proof that an arbitrary initially analytic shape remains analytic, even for short times, though computational results suggest this at least for some class of initial conditions. The only global result is for a near-circular interface without any sink or source (Constantin & Pugh 1993). There are also no exact time-evolving solutions that shed a light on the expected singular limit $\mathscr{B} \to 0^+$. Even computationally, the problem remains very challenging in this limit, though many advances have been made in computational algorithms (see for example DeGregoria & Schwartz 1985; Hou, Lowengrub & Shelley 1994; Kelly & Hinch 1997) and computer capabilities.

In an effort to understand this limit, an asymptotic procedure was proposed (Tanveer 1993) for small $\mathscr{B}$. It starts with an extension of the domain to at least part of the complex plane, where initial data are specified This makes the initial value problem well-posed, even for $\mathscr{B} = 0$ (see Baker, Segel & Tanveer 1995), unlike the problem of interfacial evolution for $\mathscr{B} = 0$. Since the $\mathscr{B} = 0$ problem in the

extended domain is well-posed, it was argued (Tanveer 1993) that a valid asymptotic expansion procedure for small $\mathscr{B}$ necessarily required this extended complex-plane domain. However, this presents very challenging mathematical difficulties since the theory of higher-order partial differential equation in the complex spatial domain is quite undeveloped. Until very recently (Costin & Tanveer 1999), no general theory existed for the existence and uniqueness of such solutions. Nonetheless, despite the fact that many mathematical issues need to be resolved, the asymptotic results give at least an indication of some features of the limiting dynamics both for Hele-Shaw (Tanveer 1993; Siegel *et al.* 1996) and two-dimensional dendritic crystal growth (Kunka, Foster & Tanveer 1997, 1999).

The discussion of the initial value problem in this paper will be limited to the question of whether a smoothly evolving $\mathscr{B} = 0$ (idealized) interface shape is necessarily the limiting solution as $\mathscr{B} \to 0^+$ at least for $O(1)$ time. Based on the evidence so far (Siegel *et al.* 1996; Ceniceros & Hou 2000), the answer is negative. There exists some family of initial conditions for which the shape corresponding to the limiting solution veers dramatically from the corresponding idealized shape in $O(1)$ time. We briefly discuss how this follows from the equations in the extended domain.

Through analytical continuation of boundary conditions (77) and (78), through a process similar that in § 5, one obtains a nonlinear integro-differential equation (Tanveer 1993):

$$z_t = q_1 z_\zeta + q_2 + \mathscr{B} q_3 + \mathscr{B} \frac{q_4}{z_\zeta{}^{1/2}} + \mathscr{B} \frac{q_5 z_{\zeta\zeta}}{z_\zeta{}^{3/2}} - 2\mathscr{B} q_7 \left[z_\zeta^{-1/2} \right]_{\zeta\zeta} \tag{81}$$

where each of q_1 to q_7 are analytic functions everywhere in $|\zeta| > 1$ and can be expressed as integrals of z_ζ (see Tanveer 1993 for details) and $z_{\zeta\zeta}$ in the physical domain. If one seeks a formal asymptotic expansion

$$z \sim z_0 + \mathscr{B} z_1 + \cdots \tag{82}$$

then

$$z_{0t} = q_{1_0} z_{0\zeta} + q_{2_0} \tag{83}$$

where subscript 0 refers to simplifications of the q_i due to the substitution of the $\mathscr{B} = 0$ solution. Polubarinova-Kochina (E. Yu. Hohlov, private communication) apparently was the first to derive (83) for $\mathscr{B} = 0$. Similarly, the next-order perturbation term z_1 satisfies

$$z_{1t} - q_{1_0} z_{1\zeta} - q_{1,1} z_{0_\zeta} = -2 q_{7_0} \left[z_{0\zeta}^{-1/2} \right]_{\zeta\zeta}. \tag{84}$$

Because of the analytic nature of q_1 and q_2 in $|\zeta| > 1$, each singularity $\zeta_s(t)$ of z_0 present at the initial time moves with velocity determined by

$$\dot{\zeta}_s = -q_{1,0}(\zeta_s(t), t). \tag{85}$$

There is an important property crucial property (Tanveer 1993) that

$$\operatorname{Re} \frac{q_{1_0}}{\zeta} > 0 \tag{86}$$

for $|\zeta| > 1$, which immediately implies from (83) that all information including singularities moves inwards towards the unit circle. This follows from noticing the analyticity of q_{1_0} and use of characteristics.

A zero $\zeta_0(t)$, defined as a point where $z_{0_\zeta} = 0$ but z_0 is otherwise analytic, is also significant. If such a point, initially outside the unit ζ-circle, strikes $|\zeta| = 1$ later in

time, it causes a zero-angled cusp at the interface that protrudes into the viscous fluid. From (83), it can be deduced that a simple (generically the case) zero moves in accordance with

$$\dot{\zeta}_0(t) = -q_{1_0}(\zeta_0(t), t) + \frac{q_{2,0_\zeta}}{z_{0_{\zeta\zeta}}}. \tag{87}$$

Comparing (85) and (87), we note $\zeta_0(t)$ would move at a different speed than a singularity $\zeta_s(t)$, if it were at the same location. This difference is significant, as will be shortly argued.

Consider equation (84) for z_1. As we approach a zero $\zeta_0(t)$, $z_{0_\zeta} \sim z_{0_{\zeta\zeta}}(\zeta_0(t), t)(\zeta - \zeta_0(t))$. This causes a singular forcing on the right of (84) at $\zeta_0(t)$. This induces a singularity in $z_1(\zeta, t)$ at $\zeta_0(t)$ and its behaviour as this point is approached is given by

$$z_1(\zeta, t) \sim A_0(t)(\zeta - \zeta_0(t))^{-5/2} \tag{88}$$

where $A_0(t)$ is determined completely terms of z_0 (see (4.8) in Tanveer 1993), with $A_0(0) \neq 0$. For an initial condition, independent of $\mathscr{B}$,

$$z_1(\zeta, 0) = 0. \tag{89}$$

Therefore, (88) cannot be uniformly valid as $t \to 0^+$, since it is inconsistent with (89). The singularity (88) must disappear as $t \to 0^+$, but it does not for (88), since $A_0(0) \neq 0$. To get a uniformly valid asymptotic behaviour of z_1 near $\zeta_0(t)$ for all time, we are forced to add a solution to the associated homogeneous equation (84). The homogeneous equation allows a solution with singular behaviour

$$A_1(t)(\zeta - \zeta_d(t))^{-5/2},$$

where

$$\dot{\zeta}_d(t) = -q_{1_0}(\zeta_d(t), t) \quad \text{with } \zeta_d(0) = \zeta_0(0), \quad A_1(0) = -A_0(0), \tag{90}$$

and $A_1(t)$ evolves according to some differential equation and is determined (equation 4.10 in Tanveer 1993). By adding this singular term to (88), we obtain as $\zeta \to \zeta_0(t)$, a uniformly valid expression for all $t > 0$:

$$z_1(\zeta, t) \sim A_0(t)(\zeta - \zeta_0(t))^{-5/2} + A_1(t)(\zeta - \zeta_d(t))^{-5/2}. \tag{91}$$

The last term in (91) ensures consistency with initial condition (89). The point $\zeta_d(t)$ has been referred to as the 'daughter singularity' since for $t = 0$ it coincides with a zero $\zeta_0(0)$; yet for $t > 0$, due to the differing speed of motion of a zero $\zeta_0(t)$ (as given in (87)) and the daughter singularity (as given by (90)), the two points are separated. Generally, for $t > 0$, until the time $\zeta_d(t)$ hits the unit circle $|\zeta| = 1$, it defines a point in the complex plane where the asymptotic expansion (82) is inconsistent because z_1 is singular. Indeed, it is easily argued that z_2, z_3, etc. are progressively more singular. Thus, a secondary 'inner expansion' is necessary in a neighbourhood of $\zeta_d(t)$, in the same way as around a zero $\zeta_0(t)$ or any singularity $\zeta_s(t)$ of z_0. It is important to note that $\zeta_d(t)$ is neither a zero nor a singularity of z_{0_ζ}, yet the assumed asymptotic expansion (82) cannot be consistent in a small neighbourhood of $\zeta_d(t)$. Earlier, based on Domb–Sykes plots, numerical calculations of Dai, Kadanoff & Zhou (1991) suggested that an initial zero breaks up into other structures, whose form remained unclear. Formal asymptotic arguments are presented in Tanveer (1993), which have since been expanded (Siegel *et al.* 1996) to include the case when $\zeta_d(t)$ is near $|\zeta| = 1$. According to these arguments,

1. Before $\zeta_d(t)$ comes very close to $|\zeta| = 1$, it defines the centre of a cluster of $-4/3$ singularities of z_ζ, with the cluster size scaling as $\mathscr{B}^{1/3}$.

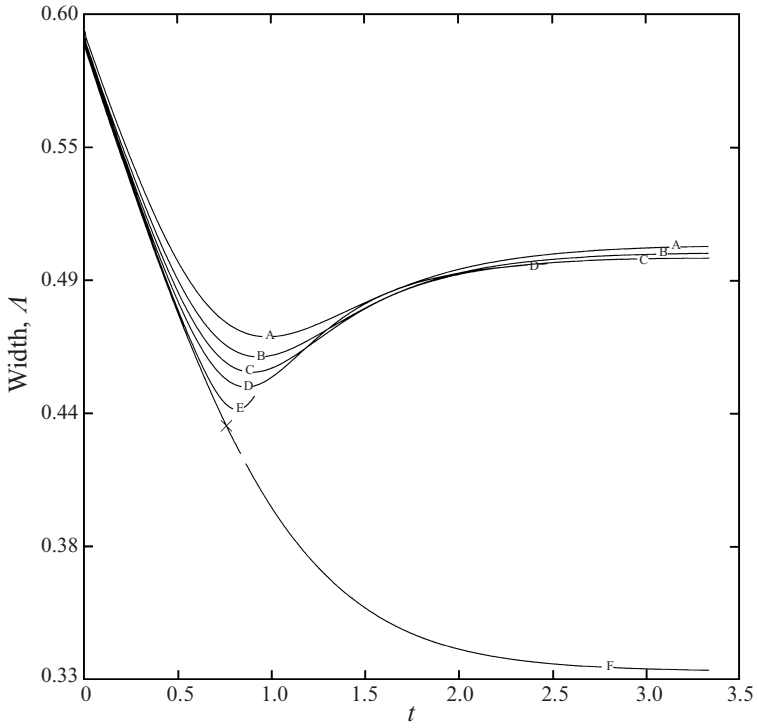

FIGURE 11. Evolution of inverse tip velocity Λ for different $\mathscr{B}$.

2. In some cases, ζ_d can impact $|\zeta| = 1$ at a time $t = t_d$, before any other singularity or zero of z_{0_ζ}. Whether this is the case or not can be determined from the differential equation (90), which can be solved from knowing only the corresponding $\mathscr{B} = 0$ solution. However, not all initial conditions lead to a daughter singularity impact preceding the approach of some other singularity or zero (see Hinch & Kelly 1997 for instance).

3. For cases where 2 is applicable, the first time, t_{impact}, when $\mathrm{Max}\,|z_\zeta - z_{0_\zeta}| = O(1)$ is given by $t_{impact} = t_d + O(\mathscr{B}^{1/3})$. Beyond t_{impact}, the actual interfacial shape veers away from the corresponding $\mathscr{B} = 0$ (idealized) shape, even though the latter is free from any high-curvature region.

4. The initial impact is followed by break-up of the 'daughter' singularity cluster into sub-clusters that advect away from the finger tip towards the tails.

5. Numerical evidence (Siegel *et al.* 1996) shows that the daughter singularity impact on a narrow finger is followed by a fattening of the finger, until a steady ZST finger shape with selected finger width emerges (see figure 11).

It is to be noted that without the excursion in the complex plane, there is no way to detect the 'daughter' singularity effect. It is clear that the results suggest that regardless of how small surface tension is, it is not always correct to assume that surface tension effects are not significant in $O(1)$ time when the corresponding idealized solution is smooth and free of large curvature. We may ask how an arbitrarily small surface tension times a curvature that is estimated to be $O(1)$, can lead to a significantly different interface shape from the corresponding idealized solution. What is ignored in this argument is that the actual interface curvature is not the same as the curvature predicted by the idealized solution. From a mathematical perspective, this

is not unexpected. The idealized problem is structurally unstable, so no continuity of the solution can be expected when we change the parameter from $\mathscr{B} = 0$ by a little. Further, the initial value problem is ill-posed when $\mathscr{B} = 0$, hence the solution operator is unbounded (in an appropriate norm). This means that small regularization such as a non-zero surface tension, changes the solution operator in an uncontrolled manner. In the following section, we demonstrate more explicitly how a 'daughter singularity' effect arises in a model partial differential equation that in many respects is similar to (81).

8. Illustrative example of daughter singularity effects

We consider a relatively simple partial differential equation in the complex lower half-ξ-plane:

$$G_t + \mathrm{i}G_\xi = 1 + 2\mathrm{i}\mathscr{B}\left[G^{-1/2}\right]_{\xi\xi\xi}. \tag{92}$$

We assume that the domain of physical interest is the real ξ-axis and the upper half-ξ-plane. Aside from the cosmetic differences of the domain (upper half-ξ-plane versus the interior of the unit ζ-circle), this equation is similar in some respects to the equation for z_ζ, obtained by differentiating (81), except that the non-local analytic terms q_j have been replaced by constants while only the most singular surface tension term retained. G is similar to z_ζ in (81). Earlier, Constantin & Kadanoff (1991) had used a localized approximation of the Hele-Shaw dynamics, valid only for a nearly circular interface, to obtain equations quite similar to (92). We will assume here that $\mathscr{B} \ll 1$. We start with an initial condition

$$G(\xi, 0) = 1 - 2\mathrm{i}\xi. \tag{93}$$

Then the solution $G^0(\xi, t)$ corresponding to $\mathscr{B} = 0$ is clearly given by

$$G^0(\xi, t) = 2\mathrm{i}(\xi_0(t) - \xi) \tag{94}$$

where

$$\xi_0(t) = -\frac{\mathrm{i}}{2}(1 - t). \tag{95}$$

Clearly, $\xi_0(t)$ is a zero of $G^0(\xi, t)$ in the lower-half complex-ξ-plane for $t \in (0, 1)$ and only strikes the real axis at $t = 1$. Before that time, it would appear reasonable to assume that at least on the real axis,

$$G(\xi, t) \sim G^0(\xi, t) + \mathscr{B}G^1(\xi, t) + \cdots. \tag{96}$$

The asymptotic expansion (96), however, cannot be valid at the complex point $\xi_0(t)$ since $G^0 = 0$ at that point, which means that regardless of how small $\mathscr{B}$ is, $\mathscr{B}[G^{0^{-1/2}}]_{\xi\xi\xi}$ is not small in some neighbourhood of $\xi_0(t)$. It is clear, therefore, that the asymptotics (96) is invalid in some region around $\xi_0(t)$, where one might expect a secondary inner expansion that matches to (96). Actually, when $t = O(\mathscr{B}^{2/7})$, the existence and uniqueness of analytic solutions to (92) for $\mathrm{Arg}\,[\mathrm{i}(\xi_0(t) - \xi)] \in (-4\pi/9, 4\pi/9)$ with the asymptotic matching condition $G(\xi, t) \sim G^0(\xi, t)$ for $\mathscr{B}^{-2/7}(\xi - \xi_0(t)) \gg 1$ has been proved (see Example 2, Costin & Tanveer 1999).† For later times, $\xi_0(t)$ moves towards the real axis, but for $t \in (0, 1)$, there would seem no good reason to suspect that (96) is invalid on the real ξ-axis. We will determine explicitly that this assumption is

† To exactly obtain Example 2 of Costin & Tanveer (1999), we rescale $\mathrm{i}(\xi_0(t) - \xi) = 2^{-1/7}\mathscr{B}^{2/7}x$, $G = \mathscr{B}^{2/7}2^{6/7}H^{-2}$ and $t = \mathscr{B}^{2/7}2^{6/7}\tau$.

incorrect. On substituting (96) into (92), it follows that $G^1(\xi,t)$ satisfies

$$G^1_t + \mathrm{i}G^1_\xi = 30(2\mathrm{i}\xi_0(t) - 2\mathrm{i}\xi)^{-7/2}. \tag{97}$$

Using the relation (95), it is clear that a particular solution to (97) is given by

$$G^1_p(\xi,t) = -12[2\mathrm{i}\xi_0(t) - 2\mathrm{i}\xi]^{-5/2}. \tag{98}$$

However, this is not consistent with the imposed initial condition on $G(\xi,0)$, which implies $G^1(\xi,0) = 0$. Therefore, one must add to (98) a solution to the homogeneous part of (97) so as to satisfy this initial condition. It is then clear that

$$G^1(\xi,t) = -12[2\mathrm{i}\xi_0(t) - 2\mathrm{i}\xi]^{-5/2} + 12[2\mathrm{i}\xi_d(t) - 2\mathrm{i}\xi]^{-5/2} \tag{99}$$

where

$$\xi_d(t) = \xi_0(0) + \mathrm{i}t = -\frac{\mathrm{i}}{2} + \mathrm{i}t. \tag{100}$$

Notice that the initial zero $\xi_0(0)$ gave rise to a new singular point $\xi_d(t)$ of $G^1(\xi,t)$, where the leading-order solution $G^0(\xi,t)$ is neither singular nor zero. This point $\xi_d(t)$ behaves like the point $\zeta_d(t)$ for the Hele-Shaw problem. It is not very difficult to see that at this daughter singularity $\xi_d(t)$, the higher-order perturbation terms $G^{(2)}$, $G^{(3)}$, etc. are progressively more and more singular and therefore the asymptotic expansion breaks down in a small neighbourhood of $\xi_d(t)$. Since $\xi_d(t)$ strikes the real ξ-axis at time $t_d = 1/2$, the hypothesis that we have an asymptotic expansion of the type (96) at least on the real axis becomes invalid beyond $t = t_d$.

However, $\xi_d(t)$ itself need not be an actual singularity of $G(\xi,t)$, though it is for the terms G^1, $G^{(2)}$, etc. of the outer-asymptotic expansion (96). Since this asymptotic expansion is itself invalid near $\xi_d(t)$, it is to be expected that $\xi_d(t)$ defines the centre of some inner region where dependent and independent variables have to be rescaled before asymptotic limit $\mathscr{B} \to 0^+$ is taken. From formal arguments made previously in the Hele-Shaw context (see § 7 in Tanveer 1993), after a short initial transient when $t = O(\mathscr{B}^{2/7})$, where the inner regions around $\xi_0(t)$ and $\xi_d(t)$ and $\xi_0(t)$ coincide, it is to be expected that as $\mathscr{B} \to 0^+$, with $\xi - \xi_d(t) = O(\mathscr{B}^{1/3})$, $G(\xi,t)$ asymptotes to the similarity solution

$$G(\xi,t) \sim tM^{-2}\{\mathscr{B}^{-1/3}[-\mathrm{i}(\xi - \xi_d(t))]t^{1/6}\} \tag{101}$$

where $M(\eta)$ satisfies

$$-\tfrac{1}{2}M + \tfrac{1}{6}\eta M' = \left[-\tfrac{1}{2} + M'''\right] M^3 \tag{102}$$

with asymptotic far-field condition

$$M(\eta) \sim 1 + a_6\eta^{-6} + \cdots \tag{103}$$

in some wide-enough complex sector for some non-zero constant a_6 (see § 6 in Tanveer 1993). Since $M(\eta)$ has a string of 2/3-singularities (computed in Tanveer 1993), it follows that a $\mathscr{B}^{1/3}$ neighbourhood of $\xi_d(t)$ will contain a cluster of $-4/3$-singularities of G. The cluster of actual singularities of G also rule out an alternative ansatz on scalings in the inner region around $\xi_d(t)$. However, unlike the non-local Hele-Shaw equations (81) where the global integral terms provide a mechanism to slow down singularities and disperse them (Siegel *et al.* 1996), the daughter singularity cluster for these local equations does not break-up beyond $t = t_d = \frac{1}{2}$. This is consistent with the Constantin–Kadanoff (1991) rigorous results on the analyticity strip width estimate for their localized Hele-Shaw dynamical model, which if strictly true, would imply a finite time singularity in the physical domain, even with surface tension.

Regardless of the details of the daughter singularity cluster, which are yet to be established through rigorous mathematics, our example explicitly demonstrates that the hypothesis (96) cannot possibly be valid on the real axis beyond $t = \frac{1}{2}$, when $\xi_d(t)$ strikes the real axis. This is an illustration of the so-called daughter singularity effect on the real-axis dynamics. This effect could not have been anticipated without following the dynamics in the lower-half complex-ξ-plane. This is not unexpected since equation (92) is ill-posed for $\mathscr{B} = 0$, when the domain is restricted to the real ξ-axis, but well-posed in the extended lower-half complex-plane.

9. Discussion

The surprises in the Hele-Shaw problem mentioned in this paper can be traced to the fact that the starting point of all analysis has been the zero-surface-tension solution, i.e. the idealized equation, which is relatively simple mathematically. Yet, at this point in the parameter space, the corresponding system is structurally unstable and the initial value problem is ill-posed. Therefore, continuity of solution set with respect to small changes in parameters or initial conditions is generally lost. Therefore small terms can have large effects. Also, as one approaches the idealized system in the parameter space, the relative importance of various small terms can change in very unexpected ways leading to changes in scalings. This may well explain why a theory of dendritic crystal growth which incorporates just the Gibbs–Thompson effect with anisotropic surface energy is seemingly inconsistent with experiment (see Glicksman & Marsh 1993) for small anisotropy and small surface energy. It is to be noted that other effects such as kinetic undercooling, small convection, etc. are neglected, and despite the smallness of their estimated size in many experiments, they can potentially account for changes in the theoretically predicted scalings.

Many of these effects may seem counter-intuitive. The results in the Hele-Shaw problem, as discussed in this paper, remind us about the dangers of attaching physical intuition to a problem that is structurally unstable or ill-posed. For the same reason, one cannot look for physical significance as to why most steady solutions are not selected or why the daughter singularity effects occur. The idealized solution with which one is comparing is not physically meaningful itself.

Indeed, if the mathematics of the Hele-Shaw problem were to simplify considerably at some $\mathscr{B} = \mathscr{B}_0 \neq 0$, rather than at $\mathscr{B} = 0$, then such solutions would have preserved continuity with respect to changes in $\mathscr{B}$ at $\mathscr{B}_0$. Further, at this $\mathscr{B}_0$ the solution to the initial value problem would have continuity with respect to changes in initial conditions. There would then be none of the puzzling riddles mentioned in this paper.

This paper is dedicated to Philip Saffman on the occasion of his retirement and in deep appreciation for guidance, friendship and encouragement. The author also wishes to thank many who have read and commented on this paper, including Herbert Levine, Vincent Hakim, Martine Ben Amar, Len Schwartz, Tom Hou, Dan Joseph, Darren Crowdy and Mike Siegel. This work is supported through the National Science Foundation (NSF-DMS9803358) and NASA (NAG-3-1947).

Appendix

A.1. *Proof of Lemma 1*

Before we prove lemma 1, it is convenient to prove the following Lemma:

LEMMA 3. *Let $M(\zeta)$ be an analytic function of ζ for $\mathrm{Im}\,\zeta \leqslant 0$, except possibly at the origin where M as an integrable singularity, i.e. $\int_0^\delta |M(\zeta)||\,\mathrm{d}\zeta|$ exists. Further, in the lower half-ζ-plane $|M(\zeta)| \leqslant C|\zeta|^{-\gamma}$ for $|\zeta| \geqslant 1$. Then the functions $F_1(\zeta)$ and $F_2(\zeta)$ defined as*

$$F_1(\zeta) = \mathrm{e}^{-\zeta} \int_{-\infty}^{\zeta} \mathrm{e}^{\zeta'} M(\zeta')\,\mathrm{d}\zeta', \qquad F_2(\zeta) = \mathrm{e}^{\zeta} \int_{\infty}^{\zeta} \mathrm{e}^{-\zeta'} M(\zeta')\,\mathrm{d}\zeta' \tag{A 1}$$

satisfy the following bounds for $|\zeta| \geqslant 8$ and $\mathrm{Im}\,\zeta \leqslant 0$:

$$|F_1(\zeta)| < C_1|\zeta|^{-\gamma}, \qquad |F_2(\zeta)| < C_2|\zeta|^{-\gamma} \tag{A 2}$$

for some constants C_1 and C_2.

Proof. We will only carry out the proof for F_1, since the proof for F_2 follows from very similar steps. Let $\zeta = x + \mathrm{i}y$. We deform the contour in the ζ'-plane so that $-\infty$ is joined to ζ along the straight line $\mathrm{Im}\,\zeta' = y$. Notice that

$$F_1(\zeta) = \mathrm{e}^{-x} \int_{-\infty}^{x} \mathrm{e}^{x'} M(x' + \mathrm{i}y)\,\mathrm{d}x'. \tag{A 3}$$

Now consider the three distinct cases: (i) $|y| \geqslant |x|$, (ii) $|y| < |x|$, $x < 0$, (iii) $|y| < |x|$, $x > 0$.

Consider case (i). For $|\zeta| \geqslant 8$, clearly $|y| \geqslant 2$. Then, using (A 3), it is clear that

$$|F_1(\zeta)| < C|y|^{-\gamma} \int_{-\infty}^{x} \mathrm{e}^{x'-x}\mathrm{d}x' < C_1|\zeta|^{-\gamma}.$$

For case (ii), if $|\zeta| \geqslant 8$, it is clear that $x \leqslant -2$. Then using (A 3) and (A 2), it follows that

$$|F_1(\zeta)| < C|x|^{-\gamma} \int_{-\infty}^{x} \mathrm{e}^{x'-x}\mathrm{d}x' < C_1|\zeta|^{-\gamma}.$$

For case (iii), if $|\zeta| \geqslant 8$, then it is clear that $x \geqslant 2$. It is then suitable to express

$$F_1(\zeta) = F_{1,1}(\zeta) + F_{1,2}(\zeta) + F_{1,3}(\zeta)$$

where

$$F_{1,1}(\zeta) = \int_{-\infty}^{1} \mathrm{e}^{x'-x} M(x' + \mathrm{i}y)\,\mathrm{d}x', \quad F_{1,2}(\zeta) = \int_{1}^{x/2} \mathrm{e}^{x'-x} M(x' + \mathrm{i}y)\,\mathrm{d}x',$$

$$F_{1,3}(\zeta) = \int_{x/2}^{x} \mathrm{e}^{x'-x} M(x' + \mathrm{i}y)\,\mathrm{d}x'.$$

It is clear that

$$|F_{1,1}(\zeta)| < \tilde{C}\mathrm{e}^{-x}, \quad |F_{1,2}(\zeta)| < \mathrm{e}^{-x/2} C \int_{1}^{x/2} x'^{-\gamma}\mathrm{d}x', \quad |F_{1,3}(\zeta)| < Cx^{-\gamma} \int_{x/2}^{x} \mathrm{e}^{x'-x}\mathrm{d}x'.$$

Combining the results above, it follows that in case (iii)

$$|F_1(\zeta)| < \tilde{C}_1 x^{-\gamma} < C_1|\zeta|^{-\gamma}.$$

Hence in all three cases, the lemma follows. □

Proof of Lemma 1

Clearly, if there is a solution, it must be unique since from (61)–(62), $C_1G_1(Z) + C_2G_2(Z) \to 0$ for $\operatorname{Arg} Z \in (-\pi/2, 0]$ implies $(C_1, C_2) = (0, 0)$ Now, define

$$G_{p_1}(Z) = G_1(Z) \int_{-\mathrm{i}\infty}^{Z} G_2(\xi)\,\mathrm{d}\xi.$$

Define

$$M(\zeta) = \mathrm{e}^{-\zeta} \frac{G_2(2\sqrt{\zeta})}{\sqrt{\zeta}}, \quad \zeta = Z^2/4.$$

It is clear from the asymptotics of G_2 that for ζ in the lower half-ζ-plane, with $|\zeta| \geqslant 1$,

$$|M(\zeta)| < C|\zeta|^{\alpha/2-3/4}$$

for some constant C, and that

$$G_{p_1}(Z) = G_1(Z)\mathrm{e}^{Z^2/4}F_1(Z^4/4)$$

with $F_1(z)$ as defined in the previous lemma. Applying Lemma 3, and using the property that $G_1(Z)\mathrm{e}^{Z^4/4} \sim Z^{-\alpha-1/2}$, it follows that for $|Z^2/4| \geqslant 8$, with $\operatorname{Arg} Z^2 \in (-\pi, 0)$,

$$|G_{p_1}(Z)| < C_1|Z|^{-2}.$$

Similarly, if we define

$$G_{p_2}(Z) = -G_2(Z) \int_{\infty}^{Z} G_1(\xi)\,\mathrm{d}\xi$$

it follows with the choice

$$M(\zeta) = \mathrm{e}^{\zeta} \frac{G_1(2\sqrt{\zeta})}{\sqrt{\zeta}}$$

that the corresponding F_2 is related to G_{p_2} through the relation

$$G_{p_2}(Z) = -G_2(Z)\mathrm{e}^{-Z^2/4}F_2(Z^4/4)$$

where F_2 is as defined in the previous lemma. Using lemma 3 again, with $\gamma = -\alpha/2 - 3/2$, and using the relation $G_2(Z)\mathrm{e}^{-Z^2/4} \sim Z^{\alpha-1/2}$, it follows that

$$|G_{p_2}(Z)| < C_2|Z|^{-2}$$

for $|Z|^2/4 \geqslant 8$ and $\operatorname{Arg} Z^2 \in (-\pi, 0)$. Since, from variation of parameters, $G_p(Z) = G_{p_1}(Z) + G_{p_2}(Z)$ is clearly a solution to (57), the proof of Lemma 1 follows.

A.2. *Computation of $A(\alpha)$ and determination of its zeros*

It is clear that

$$0 = G_p(Z) - \tilde{G}_p(Z) = G_1(Z)\left(\int_{-\mathrm{i}\infty}^{0} G_2(\xi)\,\mathrm{d}\xi - \int_{\mathrm{i}\infty}^{0} G_3(\xi)\,\mathrm{d}\xi + 2\mathrm{i}k\int_{0}^{\infty} G_1(\xi)\,\mathrm{d}\xi\right).$$

So

$$A(\alpha) = \left(\int_{-\mathrm{i}\infty}^{0} G_2(\xi)\,\mathrm{d}\xi - \int_{\mathrm{i}\infty}^{0} G_3(\xi)\,\mathrm{d}\xi + 2\mathrm{i}k\int_{0}^{\infty} G_1(\xi)\,\mathrm{d}\xi\right).$$

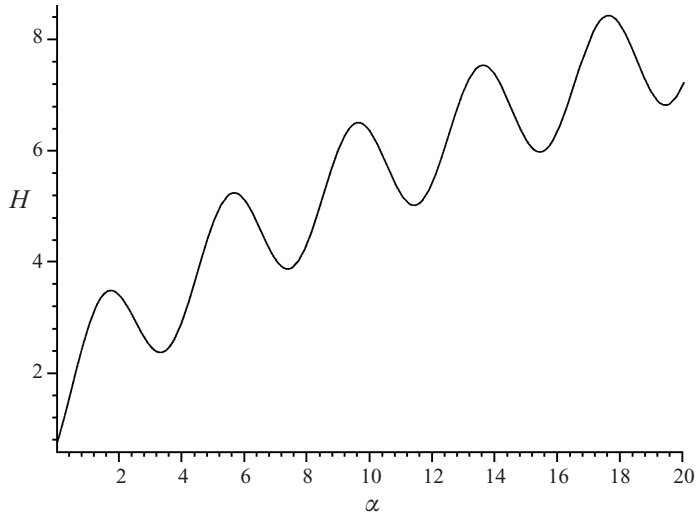

FIGURE 12. $H(\alpha)$ versus α for $\alpha \geqslant 0$.

Thus $A(\alpha)$ has to be zero for a solution to exist. Using the relations (59), we obtain

$$A(\alpha) = \cos(\pi(\alpha - 1/2)/2) \int_0^\infty U(-\alpha, r)\,\mathrm{d}r + \frac{1}{\sqrt{2\pi}} \Gamma(\alpha + 1/2)\cos(\pi\alpha) \int_0^\infty U(\alpha, r)\,\mathrm{d}r = 0. \tag{A 4}$$

This is a transcendental equation for the determination of α. We define

$$F(\alpha) = \int_0^\infty U(\alpha, r)\,\mathrm{d}r;$$

$F(\alpha)$ can be evaluated in terms of hypergeometric functions and is always positive for any α. It is known that as $\alpha \to \infty$

$$F(\alpha) \sim 2^{-1/2}\alpha^{-3/4}\mathrm{e}^{1/4+\alpha/2}(1/2+\alpha)^{-\alpha/2},$$

$$F(-\alpha) \sim \sqrt{2\pi}\mathrm{e}^{-\alpha/2-1/4}(\alpha+1/2)^{\alpha/2}\alpha^{-1/4}.$$

For $\alpha \geqslant 0$, it is convenient to rewrite (A 4) as

$$\sqrt{\frac{2}{\pi}} F(\alpha)\cos\left(\frac{\pi\alpha}{2} - \frac{\pi}{4}\right)\Gamma(\alpha+1/2)\left\{H(\alpha) + \sin\left(\frac{\pi}{4} - \alpha\frac{\pi}{2}\right)\right\} = 0 \tag{A 5}$$

where

$$H(\alpha) = \sqrt{\frac{\pi}{2}}\frac{F(-\alpha)}{\Gamma(\alpha+1/2)F(\alpha)}.$$

In figure 12, we plot $H(\alpha)$ against α. Further, for large enough α, from the asymptotics of $F(\alpha)$ and $F(-\alpha)$ as above, and the fact that $\Gamma(\alpha+1/2) \sim \sqrt{2\pi}\mathrm{e}^{-\alpha-1/2}(\alpha+1/2)^{\alpha}$, we obtain

$$H(\alpha) \sim \sqrt{\pi}\alpha^{1/2}$$

as $\alpha \to \infty$. It is clear that $H(\alpha) > 0$ for $\alpha \geqslant 0$. Also, it is clear that $H(\alpha) < 1$ in this range only for $\alpha \in [0, 0.3\ldots)$ and in this interval $\sin(\pi/4 - \pi\alpha/2) > 0$. Thus, the transcendental equation (A 5) cannot have a root for positive α, except when the

cosine term vanishes, i.e.

$$\alpha = \alpha_n = 2n + \tfrac{3}{2} \text{ for integer } n \geqslant 0. \tag{A 6}$$

For $\alpha < 0$, we use the identity $\Gamma(1/2+\alpha)\Gamma(1/2-\alpha) = \pi/(\cos(\pi\alpha))$ to rewrite (A 4) as

$$F(-\alpha)\left\{\sin\left(\frac{\pi}{4} + \alpha\frac{\pi}{2}\right) + H(-\alpha)\right\} = 0. \tag{A 7}$$

We note that the term in (A 7) within the curly brackets is the same as in (A 5), except that α is replaced by $-\alpha$. Therefore, the previous argument about this term being non-zero for $\alpha > 0$ holds again. Therefore the only roots are those for $\alpha > 0$, given by (A 6).

REFERENCES

Abramowitz, M. & Stegun, I. 1972 *Handbook of Mathematical Functions*. Dover.

Aldusin, A. P. & Matkowsky, B. J. 1998 Instabilities, fingering and Saffman–Taylor problem in filtration combustion. *Combust. Sci. Technol.* **133**, 293.

Aldusin, A. P. & Matkowsky, B. J. 1999 Extremum principles for selection in the Saffman–Taylor finger and Taylor–Saffman bubble problems. *Phys. Fluids* **11**, 1287.

Arneodo, A., Couder, Y., Grasseau, G., Hakim, V. & Rabaud, M. 1989 Uncovering the analytical Saffman–Taylor finger in unstable viscous fingering and diffusion limited aggregation. *Phys. Rev. Lett.* **63**, 984.

Baker, G. R., Siegel, M. & Tanveer, S. 1995 A well posed numerical method to track isolated conformal map singularities in Hele-Shaw flow. *J. Comput. Phys.* **120**, 348.

Barbieri, A., Hong, D. & Langer, J. 1986 Velocity selection in the symmetric model of dendritic growth. *Phys. Rev.* A **35**, 1802.

Bataille, J. 1968 Stabilite d'un deplacement radial non miscible. *Revue Inst. Pe'trole* **23**, 1349.

Ben Amar, M. 1988 Theory of needle crystal. *Physica D* **31**, 409.

Ben Amar, M. 1992 Plumes in a Hele-Shaw cell. *Phys. Fluids* A **4**, 2641.

Ben Amar, M. 1999 Void electro-migration as a moving free boundary problem. *Physica D* **134**, 275.

Ben Amar, M., Combescot, R. & Couder, Y. 1993 Viscous fingering with adverse anisotropy – a new Saffman–Taylor Finger. *Phys. Rev. Lett.* **70**, 3047.

Ben Amar, M. & Pomeau, Y. 1986 *Eur. Phys. Lett.* **2**, 307.

Ben-Jacob, E., Godbey, R., Goldenfeld, N. D., Koplik, J., Levine, H., Mueller, T. & Sander, L. M. 1985 Experimental demonstration of the role of anisotropy in interfacial pattern formation. *Phys. Rev. Lett.* **55**, 1315.

Bensimon, D. 1986 Stability of viscous fingering. *Phys. Rev.* A **33**, 1302.

Bensimon, D., Kadanoff, L. P., Liang, S., Shraiman, B. I. & Tang, C. 1986 Viscous flow in two dimensions. *Rev. Mod. Phys.* **58**, 977.

Brener, E. & Melnikov, V. I. 1990 Two dimensional dendritic growth at arbitrary Peclet number. *J. Phys. Paris* **51**, 157.

Bretherton, F. P. 1961 The motion of long bubbles in tubes. *J. Fluid Mech.* **10**, 166.

Burgess, D. & Foster, M. R. 1990 Analysis of the boundary conditions for Hele-Shaw bubbles. *Phys. Fluids* A **2**, 1105.

Ceniceros, H. & Hou, T. Y. 2000 The singular perturbation of surface tension in Hele-Shaw flows. *J. Fluid Mech.* **409**, 251–272.

Chuoke, R. L., Meurs, P. van & Poel, C. van der 1959 The instability of slow immiscible viscous liquid-liquid displacements in permeable media. *Trans. AIME* **216**, 188.

Combescot, R. & Ben Amar, M. 1991 Selection of Saffman–Taylor fingers in the sector geometry. *Phys. Rev. Lett.* **67**, 453.

Combescot, R. & Dombre, T. 1988 Selection in the Saffman–Taylor bubble and assymmetrical finger problem. *Phys. Rev.* A **38**, 2573.

Combescot, R., Dombre, T., Hakim, V., Pomeau, Y. & Pumir, A. 1986 Shape selection for Saffman–Taylor fingers. *Phys. Rev. Lett.* **56**, 2036.

Combescot, R., Dombre, T., Hakim, V., Pomeau, Y. & Pumir, A. 1987 Analytic theory of the Saffman–Taylor fingers. *Phys. Rev.* A **37**, 1270.

Constantin, P. & Kadanoff, L. 1991 Dynamics of a complex interface. *Physica D* **47**, 450.

Constantin, P. & Pugh, M. 1993 Global Solutions for small data to the Hele-Shaw problem. *Nonlinearity* **6**, 393.

Costin, O. & Tanveer, S. 1999 Existence and uniqueness for a class of nonlinear higher order partial differential equations in the complex plane. Submitted to *Commun. Pure Appl. Maths.*

Couder, Y., Gerard, N. & Rabaud, M. 1986 Narrow fingers in the Saffman–Taylor Instability. *Phys. Rev.* A **34**, 5175.

Dai, W. S., Kadanoff, L. & Zhou, S. 1991 Interface dynamics and the motion of complex singularities. *Phys. Rev.* A **43**, 6672.

DeGregoria, A. J. & Schwartz, L. W. 1985 Finger break-up in Hele-Shaw cells. *Phys. Fluids* **28**, 2313.

Dorsey, A. T. & Martin, O. 1987 Saffman–Taylor fingers with anisotropic surface tension. *Phys. Rev.* A **35** 3989.

Duchon, J. & Robert, R. 1984 Evolution d'une interface par capillarite' et diffusion de volume. *Ann l'Inst. H. Poincare'* **1**, 361.

Fokas, A. S. & Tanveer, S. 1998 A Hele-Shaw problem and the second Painleve' transcendent. *Math. Proc. Camb. Phil. Soc.* **124**, 169.

Galin, L. A. 1945 Unsteady filtration with a free surface. *Dokl. Akad. Nauk. SSSR* **47**, 246 (in Russian).

Glicksman, M. E. & Marsh, S. P. 1993 The dendrite. In *Handbook of Crystal Growth*, vol. 1 (ed. D. T. J. Hurle). North-Holland.

Guckenheimier, J. & Holmes, P. 1986 *Nonlinear Oscillations, Dynamical Systems and Bifurcations of Vector Fields.* Springer.

Hele-Shaw, H. J. S. 1898 The flow of water. *Nature* **58**, 34.

Hill, S. 1952 Channelling in packed columns. *Chem. Engng Sci.* **1**, 247.

Hohlov, E. Yu. 1990 Time-dependent free boundary problems: the explicit solution. *MIAN Preprint*, no. 14. Steklov Institute, Moscow.

Homsy, G. M. 1987 Viscous fingering in porous media. *Ann. Rev. Fluid Mech.* **19**, 271.

Hong, D. C. & Family, F. 1988 Bubbles in the Hele-Shaw cell: pattern selection & tip perturbations. *Phys. Rev.* A **37**, 2724.

Hong, D. C. & Langer, J. S. 1986 Analytic theory for the selection of Saffman–Taylor fingers. *Phys. Rev. Lett.* **56**, 2032.

Hou, T. Y., Lowengrub, J. S. & Shelley, M. J. 1994 Removing the stiffness from interfacial flows with surface tension. *J. Comput. Phys.* **114**, 312.

Howison, S. D. 1985 *Proc. R. Soc. Edin.* A **102**, 141.

Howison, S. D. 1986 Fingering in Hele-Shaw cells. *J. Fluid Mech.* **167**, 439.

Howison, S. D. 1992 Complex variable methods in Hele-Shaw moving boundary problems. *Eur. J. Appl. Maths* **3**, 209.

Howison, S. D. 2000 A note on the two-phase Hele-Shaw problem. *J. Fluid Mech.* **409**, 243–249.

Huang, S. C. & Glicksman, M. E. 1981 Fundamentals of dendritic solidification – I. Steady state tip growth. *Acta Metall.* **29**, 701.

Ivantsov, G. P. 1948 Temperature field around a spheroidal, cylindrical and acicular crystal growing in a supercooled melt. *Dokl. Akad. Nauk. SSSR* **58**, 569 (in Russian).

Kelly, E. D. & Hinch, E. J. 1997 Numerical solutions of sink flow in the Hele-Shaw cell with small surface tension. *Eur. J. Appl. Maths* **8**, 533.

Kessler, D., Koplik, J. & Levine, H. 1986 Steady state dendritic crystal growth. *Phys. Rev.* A **33**, 3352.

Kessler, D., Koplik, J. & Levine, H. 1988 Patterned Selection in fingered growth phenomena. *Adv. Phys.* **37**, 255.

Kessler, D. & Levine, H. 1985 The theory of Saffman–Taylor fingers. *Phys. Rev.* A **32**, 1930.

Kessler, D. & Levine, H. 1986*a* Stability of finger patterns in Hele-Shaw Cells. *Phys. Rev.* A **33**, 2632.

Kessler, D. & Levine, H. 1986*b* Stability of dendritic crystals. *Phys. Rev. Lett.* **57**, 3069.

Kessler, D. & Levine, H. 1987 Discrete set selection of Saffman–Taylor fingers. *Phys. Fluids* **30**, 1246.

Kruskal, M. & Segur, H. 1991 Asymptotics beyond all orders in a model of crystal growth. *Stud. Appl. Maths* **85**, 129.

Kunka, M. D., Foster, M. R. & Tanveer, S. 1997 Dendritic crystal growth for weak undercooling. *Phys. Rev.* E. **56**, 3068.

Kunka, M. D., Foster, M. R. & Tanveer, S. 1999 Dendritic crystal growth for weak undercooling, Part II: Surface energy effects on nonlinear evolution. *Phys. Rev.* E **59**, 673.

Maxworthy, T. 1987 The nonlinear growth of a gravitationally unstable interface in a Hele-Shaw cell. *J. Fluid Mech.* **177**, 207.

Maxworthy, T. 1989 Experimental study of interface instability in a Hele-Shaw Cell. *Phys. Rev.* A **39**, 5863.

McLean, J. W. 1980 The fingering problem in flow through porous media. PhD Thesis, Applied Mathematics, CalTech.

McLean, J. W. & Saffman, P. G. 1981 The effect of surface tension on the shape of fingers in a Hele-Shaw cell. *J. Fluid Mech.* **102**, 455.

Meiron, D. 1986 Selection of steady states in the two dimensional symmetric model of dendritic growth. *Phys. Rev.* A **33**, 2704.

Mineev-Weinstein, M. 1998 Selection of the Saffman–Taylor finger width in the absence of surface tension: an exact result. *Phys. Rev. Lett.* **80**, 2113.

Mineev-Weinstein, M. & Ponce-Dawson, S. 1994 Class of non-singular exact solutions for Laplacian pattern formation. *Phys. Rev.* E **50**, 24.

Misbah, C. 1987 Velocity selection for needle crystals in the 2-D one-sided model. *J. Phys. Paris* **48** 1265.

Mullins, W. W. & Sekerka, R. F. 1963 *J. Appl. Phys.* **34**, 323.

Park, C. W. & Homsy, G. M. 1985 Two-phase displacement in Hele-Shaw cells: theory. *J. Fluid Mech.* **139**, 291.

Paterson, L. 1981 Radial fingering in a Hele-Shaw cell. *J. Fluid Mech.* **113**, 513.

Pelce, P. 1988 *Dynamics of Curved Fronts*. Academic.

Pitts, E. 1980 Penetration of fluid into a Hele-Shaw cell: the Saffman–Taylor experiment. *J. Fluid Mech.* **97**, 53.

Polubarinova-Kochina, P. Ya 1945 On the motion of the oil contour. *Dokl. Akad. Nauk. SSSR* **47**, 254 (in Russian).

Reinelt, D. A. 1987*a* Interface conditions for two-phase displacement in Hele-Shaw cells. *J. Fluid Mech.* **183**, 219.

Reinelt, D. A. 1987*b* The effect of thin film variations and transverse curvature on the shape of fingers in a Hele-Shaw cell. *Phys. Fluids* **30**, 2617.

Romero, L. A. 1982 The fingering problem in a Hele-Shaw cell. PhD thesis, Department of Applied Mathematics, California Institute of Technology.

Saffman, P. G. 1986 Viscous fingering in a Hele-Shaw cell. *J. Fluid Mech.* **173**, 73.

Saffman, P. G. 1959 Exact solutions for the growth of fingers from a flat interface between two fluids in a porous medium or Hele-Shaw cell. *Q. J. Mech. Appl. Maths* **12**, 146.

Saffman, P. G. 1982 *Fingering in a Porous Medium* (ed. Burridge *et al.*) Lecture Notes in Physics. Springer.

Saffman, P. G. & Taylor, G. I. 1958 The penetration of a fluid into a porous medium of Hele-Shaw cell containing a more viscous fluid. *Proc. R. Soc. Lond.* A **245**, 312.

Saffman, P. G. & Taylor, G. I. 1959 Cavity flows of viscous liquids in narrow spaces. In *Proc. 2nd Ann. Naval Symp. Hydrodynamics*, p. 277.

Sarkar, S. & Jasnow, D. 1987 Quantitative test of solvability theory for the Saffman–Taylor problem. *Phys. Rev.* A **35**, 4900.

Schwartz, L. W. 1986 Stability of Hele-Shaw flows – the wetting-layer effect. *Phys. Fluids* **29**, 2086.

Schwartz, L. W. & DeGregoria, A. J. 1987 Simulation of Hele-Shaw cell fingering with finite capillary number effects included *Phys. Rev.* A **35**, 276.

Shaw, B. E. 1989 Universality in selection with local perturbations in the Saffman–Taylor problem. *Phys. Rev* A **40**, 5875.

Shraiman, B. I. 1986 On velocity selection and the Saffman–Taylor problem. *Phys. Rev. Lett.* **56**, 2028.

Shraiman, B. I. & Bensimon, D. 1984 Singularities in nonlocal interface dynamics. *Phys. Rev.* A **30**, 2840.

Siegel, M., Tanveer, S. & Dai, W. S. 1996 Singular Effects of surface tension in a smoothly evolving Hele-Shaw flow. *J. Fluid Mech.* **323**, 201.

Tabeling, P. & Libchaber, A. 1986 Film draining and the Saffman–Taylor problem. *Phys. Rev.* A **33**, 794.

Tabeling, P., Zocchi, G. & Libchaber, A. 1987 An experimental study of the Saffman–Taylor instability. *J. Fluid Mech.* **177**, 67.

Tanveer, S. 1986 The effect of surface tension on the shape of a Hele-Shaw cell bubble. *Phys. Fluids* **29**, 3537.

Tanveer, S. 1987*a* New solutions for steady bubbles in a Hele-Shaw cell. *Phys. Fluids* **30**, 651.

Tanveer, S. 1987*b* Analytic theory for the selection of symmetric Saffman–Taylor finger. *Phys. Fluids* **30**, 1589.

Tanveer, S. 1987*c* Analytic theory for the linear stability of Saffman–Taylor finger. *Phys. Fluids* **30**, 2318.

Tanveer, S. 1989 Analytic theory for the selection of a two dimensional needle crystal at arbitrary Peclet number. *Phys. Rev.* A **40**, 4756.

Tanveer, S. 1990 Analytic theory for the selection of Saffman–Taylor finger in the presence of thin-film effects. *Proc. R. Soc. Lond.* A **428**, 511.

Tanveer, S. 1991 Viscous Displacement in a Hele-Shaw cell. In *Asymptotics Beyond all orders* (ed. H. Segur, S. Tanveer & H. Levine). Plenum.

Tanveer, S. 1993 Evolution of Hele-Shaw interface for small surface tension. *Proc. R. Soc. Lond.* A **343**, 155.

Tanveer, S. 1996 Asymptotic calculation of three-dimensional thin-film effects on unsteady Hele-Shaw fingering. *Phil. Trans. R. Soc. Lond.* A **354**, 1065.

Tanveer, S. & Saffman, P. G. 1987 Stability of bubbles in a Hele-Shaw cell. *Phys. Fluids* **30**, 2624.

Taylor, G. I. & Saffman, P. G. 1959 A note on the motion of bubbles in a Hele-Shaw cell and porous medium. *Q. J. Mech. Appl. Maths* **12**, 265.

Thome, H., Rabaud, M., Hakim, V. & Couder, Y. 1989 The Saffman–Taylor Instability: From the linear to the circular geometry. *Phys. Fluids* A **1**, 224.

Vanden-Broeck, J. M. 1983 Fingers in a Hele-Shaw cell with surface tension. *Phys. Fluids* **26**, 2033.

Weinstein, S. J., Dussan V., E. B. & Ungar, L. H. 1990 A theoretical study of two phase flow through a narrow gap with a moving contact line: viscous fingering in a Hele-Shaw cell. *J. Fluid Mech.* **221**, 53.

Xie, X. 2000 Rigorous results in steady finger selection in viscous fingering. PhD Thesis, The Ohio State University (in preparation).

Xu, J. J. 1991 Globally unstable oscillatory modes in viscous fingering. *Eur. J. Appl. Maths* **2**, 105.

Zocchi, G., Shaw, B., Libchaber, A. & Kadanoff, L. 1987 Finger narrowing under local perturbations in the Saffman–Taylor problem. *Phys. Rev.* A **36**, 1894.

Zhuravlev, P. 1956 *Zap Leningrad Com. Inst.* **133**, 54 (in Russian).